Acta Geodyn. Geomater., Vol. 18, No. 2 (202), 137–155, 2021
DOI: 10.13168/AGG.2021.0010
journal homepage: https://www.irsm.cas.cz/acta

ORIGINAL PAPER

LANDSLIDE SUSCEPTIBILITY ASSESSMENT ALONG THE DUBAIR-DUDISHAL SECTION OF THE KARAKORAM HIGWAY, NORTHWESTERN HIMALAYAS, PAKISTAN

Javed IQBAL[1, 2, 3] *, Cui PENG [1, 3, 4] *, Mian Luqman HUSSAIN [5)], Hamid Reza POURGHASEMI [6)], Cheng DE-QIANG [1)], Safeer Ullah SHAH [5)] and Biswajeet PRADHAN [7, 8)]

[1)] *Key Laboratory of Mountain Hazards and Earth Surface Process, Institute of Mountain Hazards and Environment, Chinese Academy of Sciences, Chengdu, 610041, China.*
[2)] *Department of Earth Sciences, The University of Haripur, Haripur, 22620, Pakistan*
[3)] *China-Pakistan Joint Research Centre on Earth Sciences, Chinese Academy of Sciences, Islamabad, Pakistan*
[4)] *University of Chinese Academy of Sciences, Beijing, China.*
[5)] *National Center of Excellence in Geology, University of Peshawar, Peshawar, Pakistan*
[6)] *Department of Natural Resources and Environmental Engineering, College of Agriculture, Shiraz University, Shiraz, Iran.*
[7)] *The Centre for Advanced Modelling and Geospatial Information Systems (CAMGIS), Faculty of Engineering and IT, University of Technology Sydney, 2007 New South Wales, Australia.*
[8)] *Department of Energy and Mineral Resources Engineering, Choongmu-gwan, Sejong University, 209 Neungdong-ro Gwangjin-gu, 05006 Seoul, South Korea.*

**Corresponding author's e-mail:* javediqbalgeo@gmail.com; pengcui@imde.ac.cn

ARTICLE INFO

Article history:
Received 5 December 2020
Accepted 9 March 2021
Available online 6 April 2021

Keywords:
Karakoram Highway
Weights of evidence
Frequency ratio
Landslide susceptibility

ABSTRACT

The primary objective of this study is to analyze and characterize landslides in North Pakistan along Karakoram Highway (KKH) to produce a landslide susceptibility map using GIS and remote sensing technology. Using satellite images followed by field investigations, spatial distribution of landslide database was generated. Next, an integrated study was undertaken in the study area to perform the landslide susceptibility mapping. Dubaur-Dudishal section of KKH (about 150 km) which is a part of Kohistan Island Arc, is investigated in this study with a buffer zone of about 8 km along both sides of the KKH. Several thematic maps, e.g., lithology, distance to faults, distance to streams, distance to roads, normalized difference vegetation index (NDVI), slope, aspect, elevation, relative relief, plan-curvature and profile-curvature were prepared. Subsequently, these thematic data layers were analyzed by frequency ratio (FR) model and weights-of-evidence (WoE) model to generate the landslide susceptibility maps. In order to check the accuracy of the models, the area under the curve (AUC) was to quantitatively compare the two models used in this study. The predictive ability of AUC values indicate that the success rates of FR model and WoE model are 0.807 and 0.866, whereas the prediction rates are 0.785 and 0.846, respectively. Both methods show that nearly 50 % landslides in the study area fall in either high or very high susceptibility zones. The landslide susceptibility maps presented in this study are of great importance to the policy makers and the engineers for highway construction as well as the mega dams construction projects (Dasu dam and Bhasha dam which lie within the vicinity of the study area); so that proper prevention as well as mitigation could be done in advance to avoid the possible economic as well as the human loss in future.

INTRODUCTION

China-Pakistan Economic Corridor (CPEC) is the flagship and demonstration project of the "One Belt and One Road" strategy and it is also considered to bear the economic future of Pakistan which is attracting much attention. The Karakoram Highway (KKH) which runs parallel to sub-parallel to CPEC in North-Pakistan (in study area), was constructed in 1974-1978 and opened in 1979 usually blocks for few months every year for traffic due to the landslides. Dubair-Dudishal section of KKH (about 150 km) which is most affected by the landslides and almost half of the section is being destroyed by landslides every year (Ali et al. 2019; Ali et al. 2021). In this study, the potential slopes as well as the failed slopes along this section within a buffer zone of 8 km on both sides of the KKH were investigated through satellite images followed by field check (Figs. 1-3).

Landslides occurrence is dominantly controlled by combination of multiple factors including endogenic (or endogenetic) and exogenic (or exogenetic). The conditioning factors of slope failure include lithology, structure (e.g., folds faults, joints), slope gradient, ground water conditions and nature of the overburden (Agliardi et al., 2001, 2012; Dramis and Sorriso-Valvo, 1994). Since last two decades, landslide researchers have been using different set of parameters to predict and map the landslides prone areas on regional and local scales (e.g., Armaş, 2012; Basharat et al., 2016; Beguería, 2006; Dahal et al., 2008; Dai and Lee, 2002; Dai et al., 2001; Ding et al. 2017; Iqbal et al., 2017; Li et al., 2016; Neuhäuser et

Cite this article as: Iqbal J, Peng C, Hussain M L, Pourghasemi H R, De-qiang C, Shah S U, Pradhan B: Landslide susceptibility assessment along the Dubair-Dudishal section of the Karakoram Highway, Northwestern Himalayas, Pakistan. Acta Geodyn. Geomater., 18, No. 2 (202), 137–155, 2021. DOI: 10.13168/AGG.2021.0010

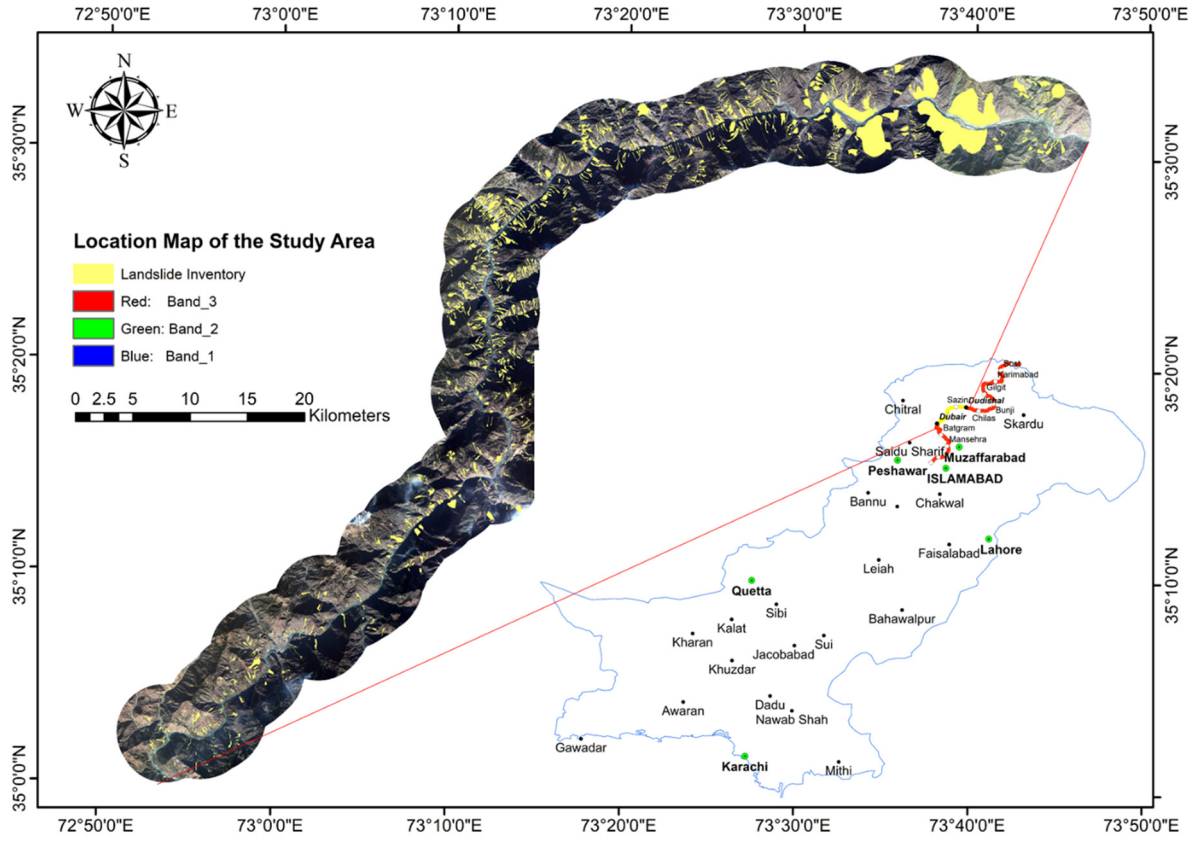

Fig. 1 Location map of the study area with landslides projected over high resolution GAOFEN-I satellite images.

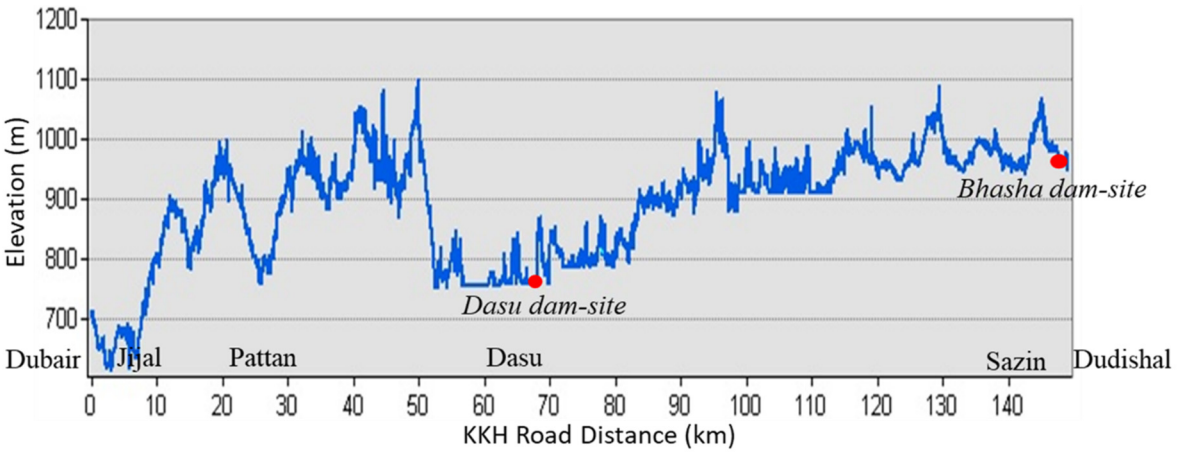

Fig. 2 Elevation profile of the KKH in study area (Dubair to Dudishal Section).

al., 2012; Poli and Sterlacchini, 2007; Pourghasemi et al., 2013a, 2013b; Prasannakumar and Vijith, 2012; Süzen and Doyuran, 2004; Van Westen et al., 2003; Xu et al., 2012a). This research still needs more work to better understand the behavior of the landslides under different internal and external conditions using different techniques (Barredo et al., 2000; Dai and Lee, 2002; Rupke et al., 1988). However, the GIS based landslide susceptibility mapping has become very convenient and reliable (Van Westen et al., 2006). Van Westen (2000) and Van Westen et al. (2003) have discussed the landslide susceptibility modelling in very detail. In this paper, landslide susceptibility of a very potential landslide segment of KKH was considered using weights-of-evidence (WoE) (Chung and Fabbri, 2003; Carranza and Hale, 2000; Lee et al., 2004; Rezaei Moghaddam et al., 2007) and the frequency ratio (FR) (Lee and Pradhan, 2007; Lee and Sambath, 2006; Mondal and Maiti, 2013; Yilmaz, 2009; Yalcin et al., 2011). Active fault system in north Pakistan exists due to continuous collision between the Eurasian and the Indian plates (Fraser et al., 2001; Khan et al., 1996; Searle et al., 1999). In north Pakistan, collision margin is characterized with the presence of two suture zones as Main Karakoram Thrust (MKT) high-grade

Fig. 3 Typical landslides in Dasu (Kohistan District) along KKH.

metamorphic rocks and the Main Mantle Thrust (MMT) along the southern edge of Kohistan Island Arc which is crammed between the two plates (Tahirkheli, 1979). The collision of northern and southern margins of the Kohistan arc with Eurasian and Indian plates had occurred at about 90 and 50 Ma, respectively (Clift et al., 2002; Hanson, 1989; Petterson and Windley, 1985; Treloar, 1997; Treloar et al., 1989, 1996, 2003). Since then, the development of Karakoram and Himalayan mountain system is in process with duplication of curst along thrust faults and lateral transition of the orogen with strike-slip faults. Although most active deformation has been predicted along the mountain fronts as in-sequence deformation, nonetheless internal part of the system is characterized with out-of-sequence deformation (Morley, 1988) with consideration of mechanics of thrusting (Davis, 1983). This is reflected by the seismicity, occurrence of great earthquakes, and presence of active faults such as Balakot-Bagh fault (Ishtiaq et al., 2015).

Despite of numerous geohazards along KKH since its construction, no significant study has been carried out on geomorphic and lithological control on landslides along KKH to investigate the correlation between the litho-morphic characters of the region and the landslide events. The rate of erosion due to active tectonic uplift increases nonlinearly with respect to the slope of topography until a threshold slope angle (maximum slope) is reached (Burbank et al., 1996; Schmidt and Montgomery, 1995). Until the topographic slope reaches the threshold, the slope angles and erosion rates increase with respect to the rate of regional uplift. In addition to this, the threshold

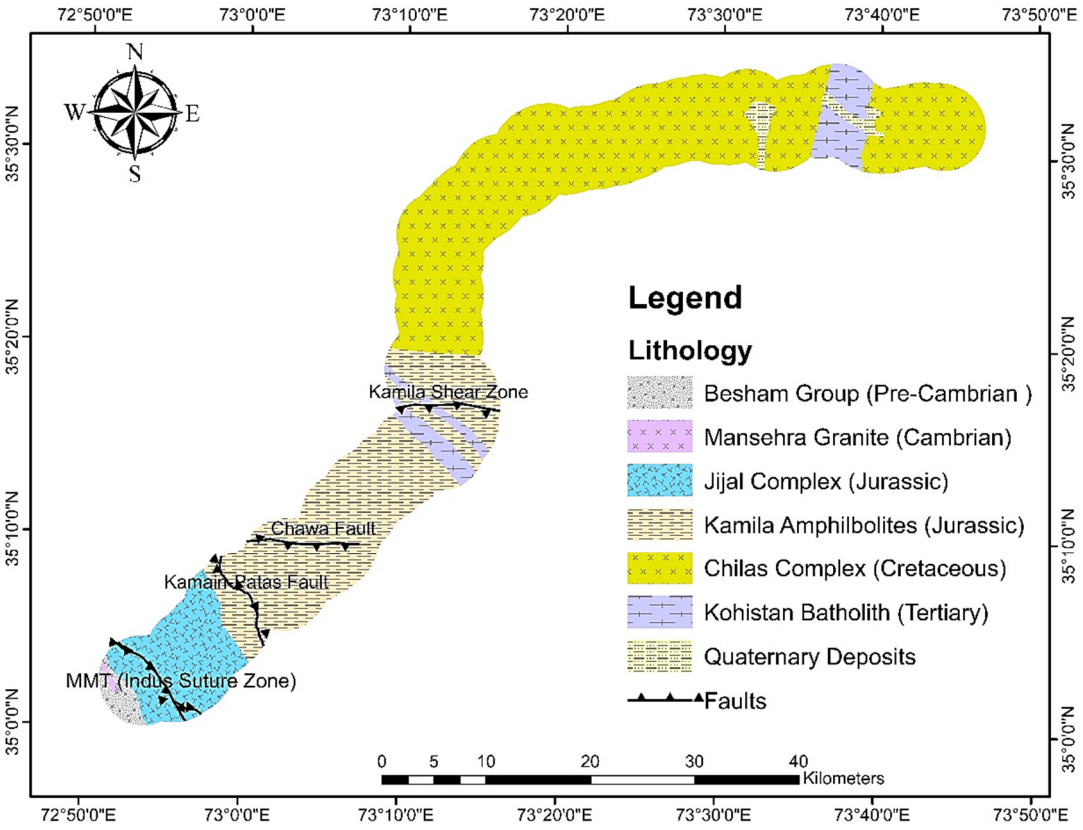

Fig. 4 Geological map of the study area.

slope angle in response to the tectonic-driven incision is mainly achieved by slope failures of the over-steepened river banks (Burbank et al., 1996; Larsen and Montgomery, 2012).

The proposed study is aimed towards the analysis of landslide phenomena along KKH region with a special emphasis on their relationship with the litho-morphic environment of the terrain to generate a landslide susceptibility maps.

STUDY AREA

The study area lies between Dubair and Dudishal towns in north-Pakistan, having a linear road distance of about 150 km with a buffer zone of 8 km on both sides of the KKH (total area of about 1200 km^2) (Figs. 1-3), including the northern part of the Indian plate (few km only and the southern part of Kohistan Island Arc / Eurasian Plate). The absolute elevation ranges from 572 m to 3545 m having all types of natural geomorphic features including rivers, mountains and valleys. The climatic conditions changes in time but remains nearly similar in space. The annual mean temperature ranges from -5 °C to 46 °C whereas the mean annual rainfall is around 1000-1500 mm which is mostly concentrated during the months of January-March and July-August (Pakistan Meteorological Department).

The lithology of the Dubair-Dudishal section is mainly composed of igneous and metamorphic rocks with exception of quaternary deposits. Six major lithologies were found in the study area including the "Besham group of Pre-Cambrian age (biotitic/ cataclastic gneisses and quartzite)", "Chilas complex of Cretaceous age", "Jijal complex of Jurassic age (Alpine type metamorphic rocks and garnet granulites)", "Kamila amphibolite of Jurassic age (amphibolites)", "Mansehra granite of Cambrian age (granites)", "Kohistan batholith of Tertiary age" and "Quaternary deposits (recent deposits)" (Fig. 4) (Ding et al., 2016; Khan et al., 1996; Searle et al., 1999; Tahirkheli and Jan, 1979; Treloar et al., 1996).

MATERIALS AND METHODS

A comprehensive study for landslides identification and analysis was carried out to better understand the landsliding along KKH taking Dubair-Dudishal section as case study. Using GAOFEN-I satellite images with a multispectral resolution of 8.5 m and the panchromatic resolution of 2.5 m followed by selected field investigations, a landslide occurrence database was generated. Thematic maps, e.g., lithology, distance to faults, distance to streams, distance to roads, NDVI, slope angle, aspect, elevation, relative relief, plan-curvature and profile-curvature were prepared using ArcGIS. Subsequently, these thematic data layers were analyzed by frequency ratio (FR) Model and weights-of-evidence (WoE) model to generate the landslide

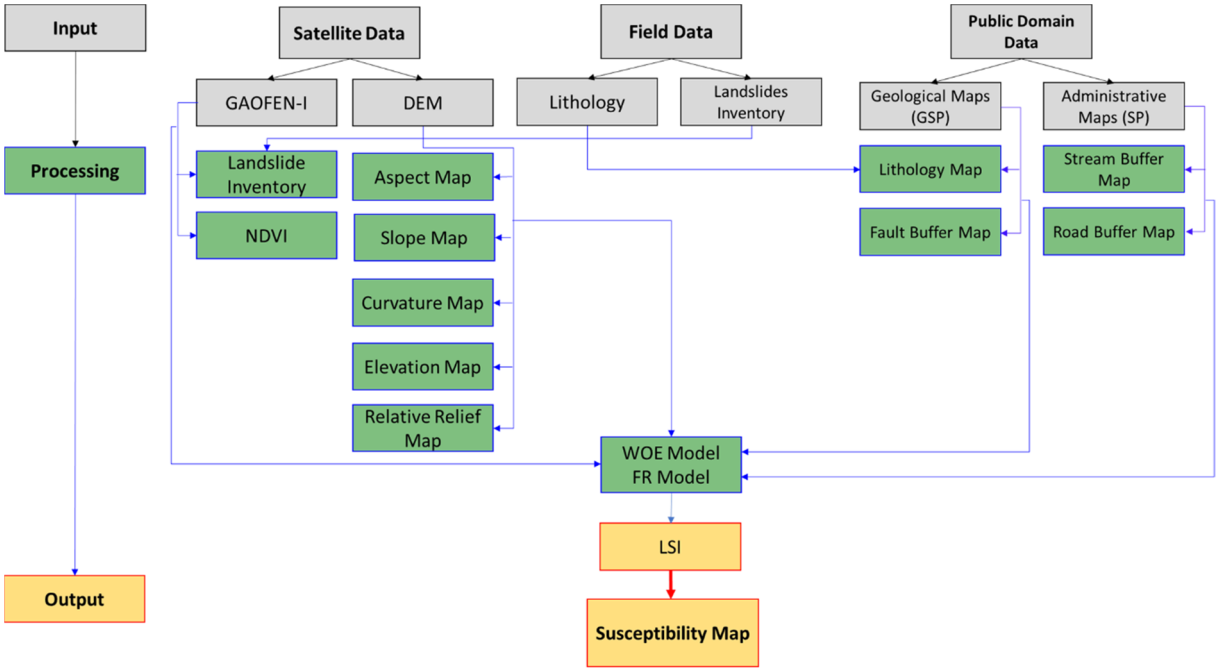

Fig. 5 Generalized flowchart of the methodology.

susceptibility maps (Fig. 5). In order to check the predictive ability, the area under the curve (AUC) was used to quantitatively compare the two models used in this study.

LANDSLIDE INVENTORY

James Hutton's theory "the present is the key to past" can be reshaped as the "past and present are the keys to the future" in landslide susceptibility and prediction. Landslides that have occurred on in the past can be used for the spatial prediction of landslides that could be occurred in the future (Varnes, 1978). The identification and preparation of landslide inventory is the most important step in susceptibility mapping. Landslide inventory is the map that shows the spatial distribution of landslides that have occurred in the past or in the present and it can be used to investigate the relationships between landslide occurrence and the various conditioning factors. A total of 1036 landslides were identified using high resolution satellite images (GAOFEN-I) followed by field check. The detailed landslide inventory based on the types of landslides (including numbers of landslides in different landslides types) using the landslide classification criteria of Cruden and Varnes (1996) is shown in Figure 6 while classification based on lithology (including number of landslides in each lithology) of the study area is shown in Figure 7.

LANDSLIDE CONDITIONING FACTORS

In order to generate the landslide susceptibility map, eleven conditioning factors were taken in this study. These factors include lithology, distance to faults, distance to streams, distance to roads, NDVI, slope, aspect, elevation, relative relief, plan-curvature and profile-curvature. The topographic parameters were derived from ALOS PALSAR derived digital elevation model (DEM) data with a resolution of 12.5 x 12.5 m. The NDVI was derived from GAOFEN-I. These multispectral and the panchromatic GAOFEN satellite images were fused in ENVI 5.3 (an image analysis software by Harris Geospatial Solutions) to get the high-resolution fused image of 2.0 m. The landslide conditioning factors layers including faults buffer, streams buffer and roads buffer were generated through Euclidean distance method. All the conditioning factors layers were produced in ArcGIS 10.5. The lithological maps provided by the Geological Survey of Pakistan (GSP) were also modified in ArcGIS 10.5 to use them in the landslide susceptibility analyses.

ELEVATION

Elevation is one of the most important conditioning factors because elevation has direct influence on the topographic parameters. The slopes at higher altitudes are more susceptible to landslide occurrence (Ercanoglu and Gokceoglu, 2002). The elevation map layer was generated from the DEM of ALOS PALSAR with 12.5 m spatial resolution. The elevation map was classified into seven categories based on the statistical analysis as well as the expert opinion (Regmi et al., 2010); i.e., <1200 m, 1200–1600 m, 1600–2000 m, 2000–2400 m, 2400–2800 m, 2800–3200 m, 3200–3600 m and >3600 m (Fig. 8-C).

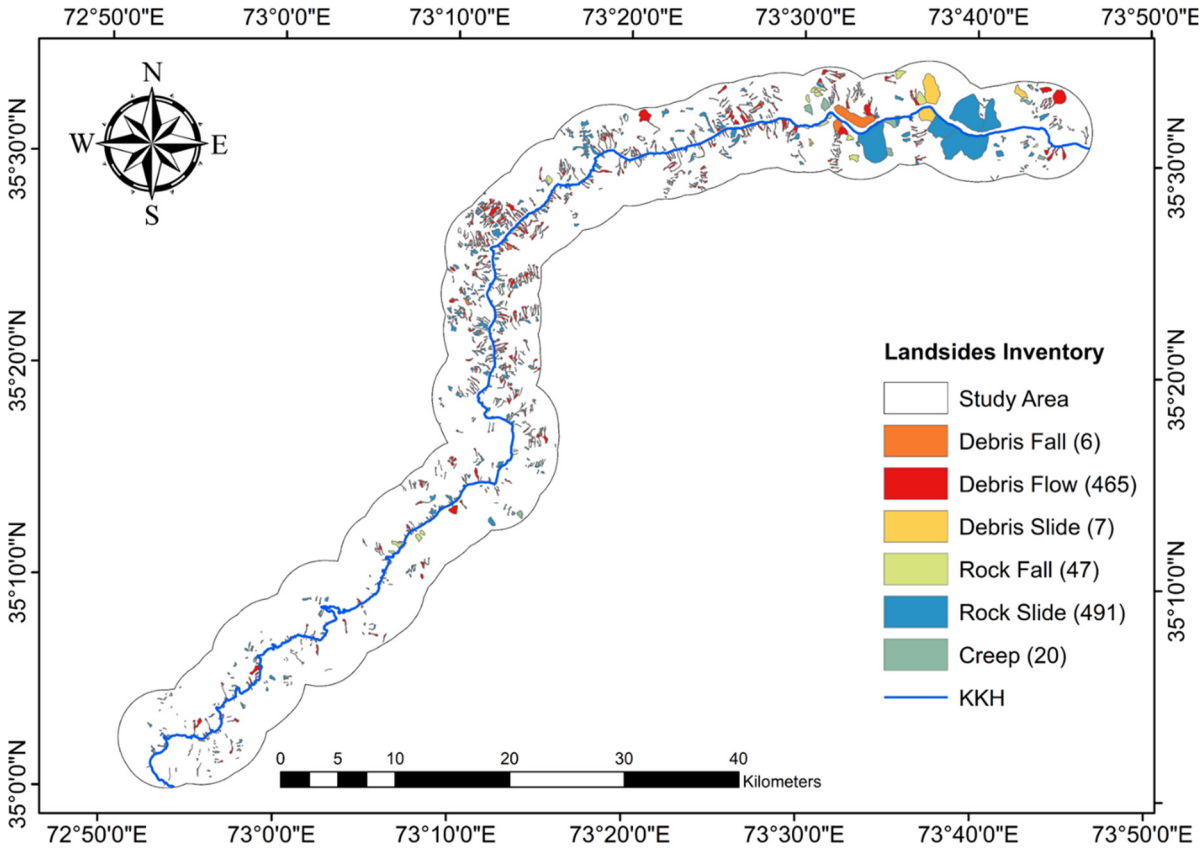

Fig. 6 Landslides inventory classification based on type of movement.

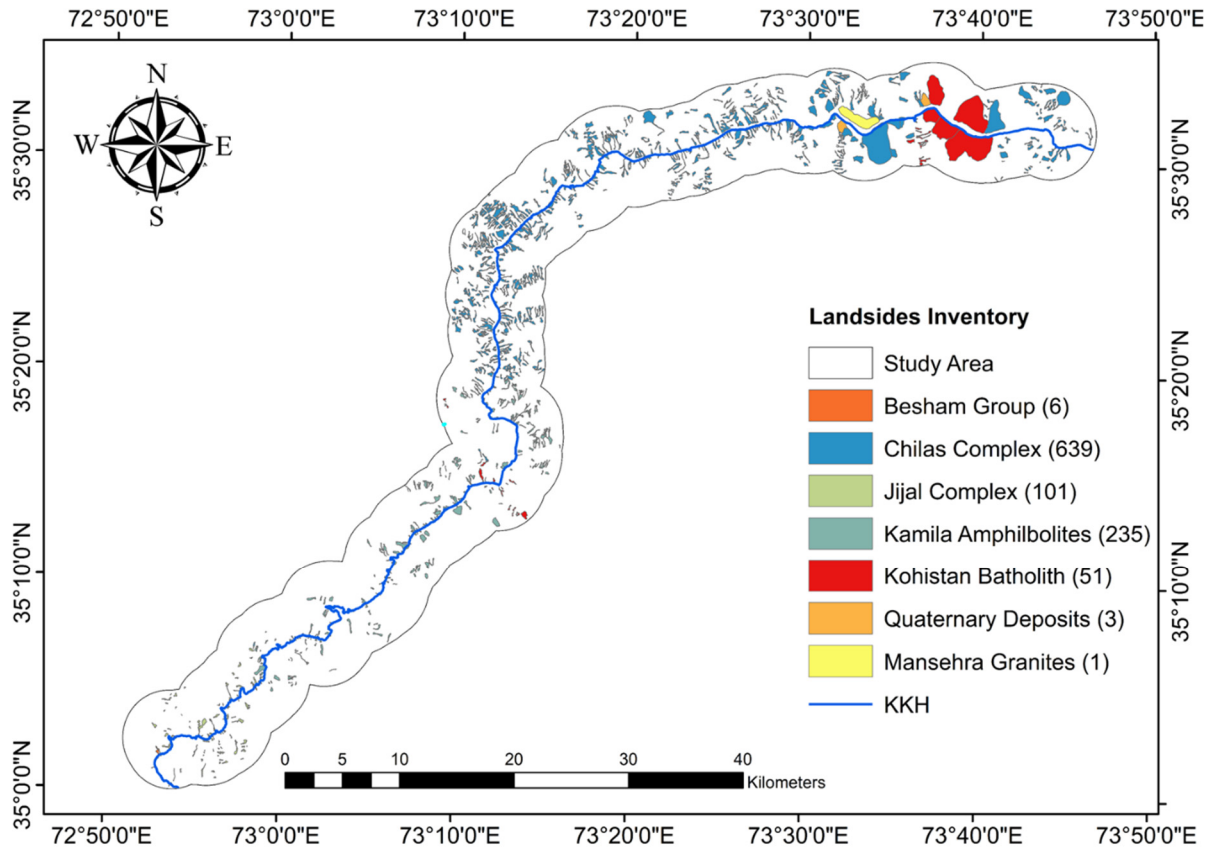

Fig. 7 Landslides inventory classification based on lithology.

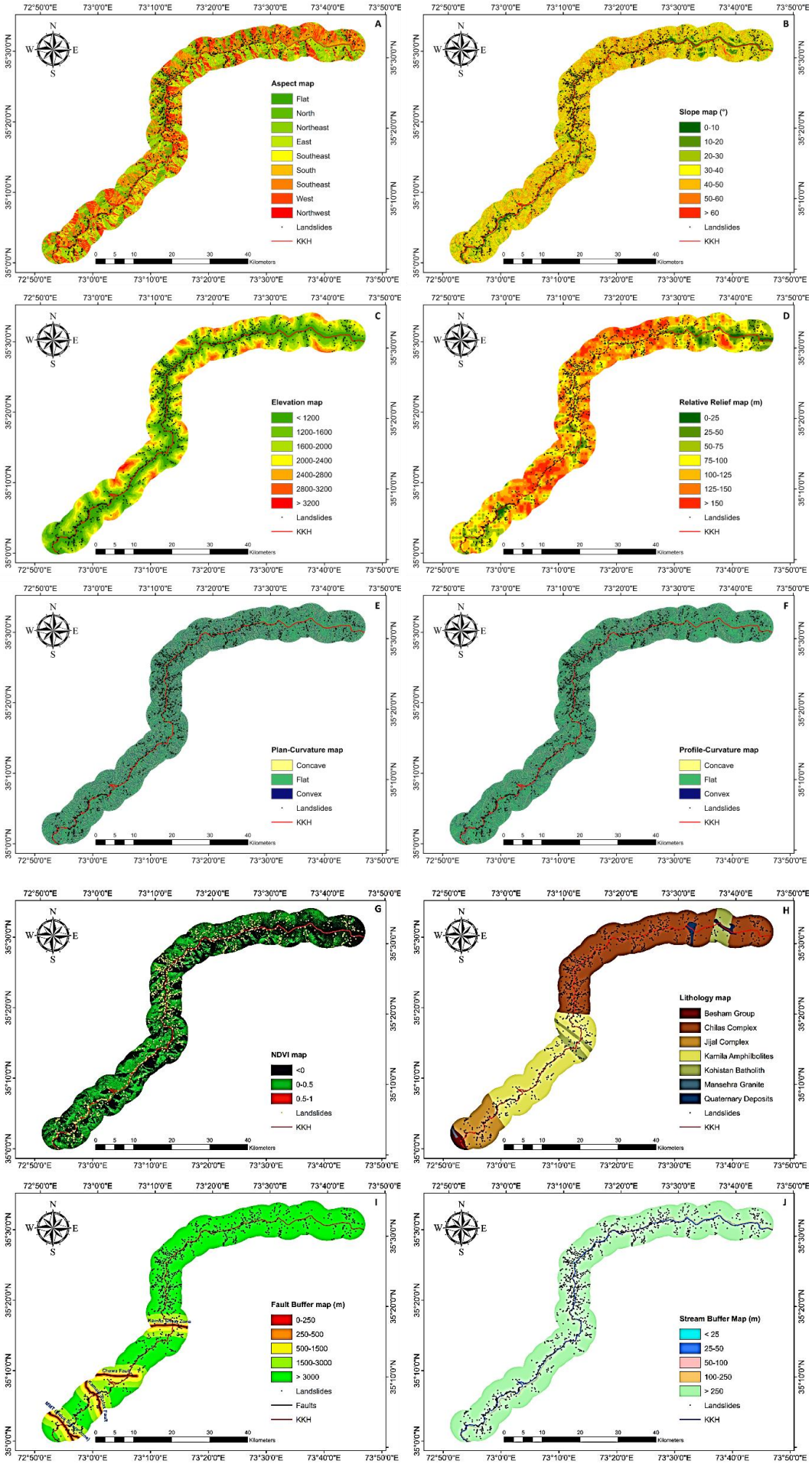

Fig. 8 Thematic maps layers of the study area used in susceptibility mapping.

RELATIVE RELIEF

Relative relief which is also known as "amplitude of available relief" or "local relief", may be defined as the difference in highest and lowest points (height) in a unit area. Relative relief is a one of the important morphometric variables which is used for the overall assessment of morphological characteristics of terrain and degree of dissection. Although relative relief does not have direct effect on the landslide occurrence, however, it controls the other factors including soil erosion, river incision and vegetation (Vijith et al., 2014). The elevation map was divided into seven categories based on the statistical analysis as well as the expert opinion; i.e., 0-25 m, 25-50 m, 50-75 m, 75-100 m, 100-125 m, 125-150 m and > 150 m (Fig. 8-D).

SLOPE ANGLE

It is another important conditioning factor of landslides. The specific contact of slope angle with friction angle, cohesion and permeability controls the slope stability. Shear forces increase with increase in slope angle which ultimately increase slope instability (Dai et al., 2001; Nefeslioglu et al., 2008; Pourghasemi et al., 2018a, 2018b). Nearly all researchers have chosen slope angle as a factor in landslide susceptibility mapping (Ayalew and Yamagishi, 2005; Yao et al., 2008). Slope layer was derived from the DEM of ALOS PALSAR with 12.5 m spatial resolution. The slope map was classified into seven categories based on the statistical analysis as well as the expert opinion; i.e., 0–10°, 10–20°, 20–30°, 30–40°, 40–50°, 50–60° and >60° (Fig. 8-B).

SLOPE ASPECT

Although there is no obvious relationship between slope aspect and landslides (Ercanoglu and Gokceoglu, 2002); however, landslides always occur in a specific direction in a particular a region (Saadatkhah et al., 2014). It may affect the slope stability through the percentage of sunshine in a day as well as hydrologic processes. The aspect layer was generated from the DEM. The aspect map was divided into nine categories; i.e., flat area, north, north-east, east, south-east, south, south-west, west and north-west (Fig. 8-A).

PLAN-CURVATURE AND PROFILE-CURVATURE

Curvature value is considered to be a topographical attribute which may be simply defined as the curves on surface (Nefeslioglu et al., 2008). In General, the curvature value increases with increase in tightness of the curve and vice versa. In this paper we have used the plan-curvature and profile-curvature for susceptibility mapping (Ayalew et al., 2004). Plan-curvature is defined as the curvature of the hillside in a horizontal plane or the curvature of the contours on a topographic map, and it controls the water flowing path. Profile-curvature is defined as the curvature of the surface in the direction of the steepest slope, and it controls the flowing speed of water (Pourghasemi et al., 2018a, 2018b; Zhou et al., 2018; Chen et al., 2017). The plan- and profile-curvature maps were generated from DEM, and were classified in to three categories; i.e., concave, flat, and convex (Figs. 8-E, F).

DISTANCE TO FAULTS

DISTANCE TO ROADS

Road construction in mountainous areas decreases the slope due to the loss of toe support due which ultimately create the tension cracks (Iqbal et al., 2018; Xu L. et al., 2014; Youssef et al., 2015). The road segment sometimes plays a role of pathway for water flow or a barrier, depending on its location within a particular area, it generally aids to the landslides (Pradhan et al., 2010; Youssef et al., 2016). Hence, distance to road is one of the important conditioning factors for landslide susceptibility mapping, especially in mountainous areas (Akgun, 2012; Pradhan, 2013). Roads buffer was classified into five buffer zones based on the statistical analysis as well as the expert opinion; i.e., 0-20 m, 20-40 m, 40-100 m, 100-350 m, >350 m (Fig. 7).

Landslides occurrence as well as their spatial distribution has direct relation with the tectono-morphic features. It is common understanding that landslides occurrence increases with decrease in distance from faults and vice versa (Xu C. et al., 2012b), it is due to the reason that faults create a lot of fractures and cracks in rocks which ultimately lower the strength of rocks and make them prone to landsliding. Hence, it has negative effects on slope stability. The faults map was extracted and reproduced in ArcGIS 10.5 from tectonic map of Geological Survey of Pakistan as well as from field observations. The distances to faults and faults buffers were made on the bases of all faults including one major fault (Main Mantle Thrust) which has a fault zone of over 1 km (Robert and David, 1988). The faults map was divided into five classes; i.e., 250 m, 500 m, 1500 m, 3000 m and >3000 m (Fig. 8-I).

DISTANCE TO STREAMS

Many researchers have considered the "distance to stream" as a main contributing factor for slope stability analysis. Presence of stream within the vicinity of the slope may have negative affect on the stability of the slope through erosion as well saturation slope (Iqbal et al., 2018). The degree of saturation has direct effect on the shear strength of slope material as well as toe erosion due to water infiltration and flow may lead to loss the support of slope. Hence, distance to streams were classified into five buffer zones based on the statistical analysis as well as the expert opinion; i.e. 0-25 m, 25-50 m, 50-100 m, 100-250 m, >250 m (Fig. 8-J).

NDVI

Normalized difference vegetation index (NDVI) is one of conditioning factors in landslide susceptibility mapping and has been considered by

many researchers. It is well understood that vegetation plays a very important role in slope stability due to its root reinforcement. The bared slopes are more susceptible to landsliding as compared to the vegetated slopes. The NDVI was derived from GAOFEN-I satellite images.

NDVI represents the total vegetation area within a particular region. The NDVI value was calculated using the following formula (Justice et al., 1985):

$$NDVI = (IR - R) / (IR + R) \quad (1)$$

where, R is red band and IR is infrared band of the electromagnetic spectrum. The NDVI was classified into three categories based on the statistical analysis as well as the expert opinion; i.e., < 0, 0-0.5 and 0.5-1 (Fig. 8-G).

LITHOLOGY

Lithology has been considered as the most important independent variable for landslide susceptibility mapping by many researchers (Akgun, 2012; Gorum et al., 2011; Peruccacci et al., 2012). Variations in lithology often lead to reduce the strength by increasing the porosity and permeability of rocks and soils (Yalcin et al., 2011). The lithological map was extracted from Geological Survey of Pakistan map and was digitized in ArcGIS. The lithology of the Dubair-Dudishal (study area) section was classified into seven lithological units; i.e., Besham group, Chilas complex, Jijal complex, Kamila amphibolite, Kohistan batholith, Mansehra granite, and Quaternary deposits (Fig. 8-H).

LANDSLIDE SUSCEPTIBILITY MAPPING

FREQUENCY RATIO MODEL

The frequency ratio (FR) model has been widely used for landslide susceptibility mapping and is endorsed by many researchers due its consistent good results in landslide susceptibility mapping (e.g., Lee and Pradhan, 2007; Lee and Sambath, 2006; Yilmaz, 2009; Yalcin et al., 2011). Mathematically it can be expresses as, (Mondal and Maiti, 2013):

$$FR = \frac{Npix(Li)/\ N\ pix(Ni)}{\sum Npix(Li)/\sum Npix(Ni)} \quad (2)$$

where, "$N_{pix(Li)}$" represents the number of pixels with landslides in class "*i",* and "$N_{pix(Ni)}$" represents the total number of pixels in a class "*i"*. Thus, the resulting value from this equation shows the correlation between the landslide and the class of independent variable. Higher value corresponds to positive relation between the conditioning factor and the landslide and the vice versa, the results were generated using different tools of ArcGIS including model builder.

The landslide susceptibility index (LSI) was calculated by addition of all classes FR values (Table 1) using the FR formula as given below (Lee and Talib, 2005; Lee and Pradhan, 2007):

$$LSI = \sum FR \quad (3)$$

The values in the calculated LSI map range from 6.53 to 13.26 (Fig. 9). In the LSI map, a higher value corresponds to a higher landslide susceptibility. Furthermore, the LSI map was reclassified into four classes using "natural break method to get the landslide susceptibility map ((i) low, (ii) moderate, (iii) high, and (iii) very high). Landslide susceptibility map show that 22 % landslides lies in low susceptibility area, 35 % landslide lie in the moderate susceptibility area, 30 % lie in the high susceptibility area and 13 % lie in the very high susceptibility area (Fig. 10).

WEIGHTS-OF-EVIDENCE MODEL

Weights-of-evidence (WoE) is an approach that works on Bayesian probability model and is being extensively used for landslide susceptibility mapping (e.g., Mohammady et al., 2012; Neuhäuser et al., 2012; Pourghasemi, 2013a, 2013b; Xu C. et al., 2012a, 2012b). "Prior" and "posterior" are the two terms which makes the base for Bayesian statistical analysis. The prior logit can be obtained from all pre-existing evidence (e.g., aspect, slope, lithology, NDVI, etc.). However, the posterior logit assumes that the initial results would be improved with the addition of other evidences. Hence, the posterior logit may be termed as the improved results obtained from landslide event of known locations in a particular class which may act as an evidence (e.g., aspect, slope, lithology, NDVI, etc.). In this study, we calculated a positive weight (W^+) for each particular predictive variable at the time of occurrence of event, and a negative weight (W-) which reflects the non-occurrence of the event, using different tools of ArcGIS including model builder. The weights measuring mathematical expressions are given below;

$$W^+ = \ln \frac{P\ (F \mid Af)}{P(F \mid \bar{A}f)} = \ln \left[\frac{\frac{\text{Landslide area in considered class}}{Total9\ landslide\ area}}{\frac{Non-landslide\ area\ in\ considerd\ class}{Total\ non-landslide\ area}} \right] \quad (4)$$

$$W^- = \ln \frac{P\ (\bar{F} \mid Af)}{P(\bar{F} \mid \overline{Af})} = \ln \left[\frac{\frac{\text{Total landslide area in other classes}}{Total\ landslide\ area}}{\frac{Total\ non-landslide\ area\ in\ other\ classes}{Total\ non-landslide\ area}} \right] \quad (5)$$

where, F is class of independent variable, whereas the overbar sign shows the absence of the class and/or landslide event.

The positive weight (W^+) is directly proportional to the occurrence of landslides (Barbieri and Cambuli, 2009). The contrast value (C) for any variable can be calculated as;

$$C = W^+ - W^- \quad (6)$$

CONDITIONAL INDEPENDENCE ANALYSIS

Conditional independence analysis was done with Chi Square method (Regmi et al., 2010; Pradhan et al., 2010). All the landslide conditioning factors were classified into binary pattern based on presence and absence criteria of the landslide using contrast weights and the expert knowledge. In general, positive weights shows the presence and vice versa.

Table 1 WoE and FR methods results of all parameters used in landslide susceptibility mapping.

Parameter Name	Parameter Class	Class Area from Total Area (%)	Landslides-affected Area in the Parameter Class (%)	W^+	W^-	C	FR
Road Distance (m)	< 20 m	0.70	1.48	0.876	-0.009	0.884	1.119
	20 – 40 m	0.66	1.31	0.796	-0.007	0.803	0.987
	40 – 100 m	1.69	2.83	0.585	-0.013	0.598	0.669
	100 – 350 m	6.95	9.39	0.338	-0.029	0.367	0.351
	> 350 m	89.99	84.99	-0.063	0.460	-0.523	0.944
Fault Distance (m)	<250	30.94	58.35	0.732	-0.546	1.278	1.886
	250 – 500 m	2.37	0.59	-1.476	0.020	-1.496	0.247
	500 – 1500 m	9.38	2.75	-1.299	0.078	-1.377	0.293
	1500 – 3000 m	13.27	5.42	-0.956	0.096	-1.052	0.408
	> 3000 m	44.03	32.89	-0.318	0.203	-0.521	0.747
Geology	Besham Group	1.30	0.18	-2.076	0.012	-2.088	0.137
	Kamila Amphilbolites	29.40	11.04	-1.042	0.259	-1.301	0.376
	Kohistan Batholith	6.46	12.26	0.740	-0.071	0.810	1.898
	Chilas Complex	50.33	65.04	0.287	-0.382	0.669	1.292
	Quaternary Deposits	1.62	8.76	2.300	-0.083	2.382	1.389
	Mansehra Granite	0.16	0.00	-1.538	0.094	-1.421	0.010
	Jijal Complex	10.53	2.72	-1.428	0.093	-1.521	0.258
Stream Distance (m)	< 25 m	0.81	0.05	-2.933	0.008	-2.941	0.058
	20 – 50 m	0.64	0.08	-2.219	0.006	-2.225	0.119
	50 – 100 m	1.34	0.60	-0.863	0.008	-0.871	0.446
	100 – 250 m	4.02	6.00	0.454	-0.023	0.477	1.493
	> 250 m	93.18	93.28	0.001	-0.015	0.016	1.001
Aspect	Flat	2.14	0.89	-0.933	0.014	0.000	0.417
	North	12.01	10.37	-0.324	0.019	-0.343	0.850
	NorthEast	12.14	12.55	0.036	-0.005	0.042	1.033
	East	11.77	9.04	-0.288	0.034	-0.322	0.768
	SouthEast	13.09	14.47	0.111	-0.018	0.128	1.105
	South	11.81	17.14	0.421	-0.069	0.489	1.451
	SouthWest	11.63	13.84	0.194	-0.028	0.222	1.190
	West	11.93	10.23	-0.168	0.021	-0.189	0.858
	NorthWest	13.46	11.46	-0.176	0.025	-0.201	0.852
Slope (°)	0 – 10°	4.38	4.53	0.038	-0.002	0.039	1.035
	10 – 20°	6.62	9.26	0.378	-0.032	0.409	1.398
	20 – 30°	17.25	18.55	0.080	-0.017	0.098	1.075
	30 – 40°	32.22	31.94	-0.010	0.005	-0.014	0.991
	40 – 50°	26.97	23.28	-0.162	0.055	-0.216	0.863
	50 – 60°	10.47	9.96	-0.055	0.006	-0.061	0.951
	> 60°	2.08	2.48	0.194	-0.004	0.198	1.190
NDVI	< 0	55.59	73.13	0.308	-0.543	0.851	1.315
	0 – 0.5	44.34	26.87	-0.541	0.306	-0.848	0.606
	0.5 – 1	0.00	0.00	-2.439	1.743	-2.439	0.005
Elevation (m)	< 1200	24.05	32.11	1.915	-0.339	2.254	1.335
	1200 – 1600 m	25.55	40.36	0.991	-0.354	1.345	1.579
	1600 – 2000 m	23.39	19.56	0.219	-0.047	0.266	0.836
	2000 – 2400 m	16.04	5.94	-0.538	0.046	-0.584	0.370
	2400 – 2800 m	8.22	1.53	-1.177	0.035	-1.213	0.186
	2800 – 3200 m	2.48	0.48	-1.370	0.014	-1.384	0.194
	> 3200 m	0.26	0.03	-2.830	0.004	-2.834	0.096
Plan-Curvature	Concave	14.44	14.61	0.869	-0.095	0.964	1.012
	Flat	58.70	62.82	0.372	-0.422	0.795	1.070
	Convex	26.85	22.58	0.577	-0.120	0.697	0.841
Profile-Curvature	Concave	11.55	9.34	3.029	-0.094	3.123	0.809
	Flat	65.18	67.77	2.264	-1.059	3.324	1.040
	Convex	23.27	22.89	1.139	-0.184	1.323	0.984
Relative Relief (m)	0 – 25 m	1.47	3.85	0.034	-0.001	0.036	2.614
	25 – 50 m	6.05	16.15	0.268	-0.044	0.312	2.671
	50 – 75 m	13.00	15.99	0.133	-0.024	0.157	1.230
	75 – 100 m	20.86	17.80	0.516	-0.084	0.599	0.853
	100 – 125 m	27.08	22.93	1.315	-0.197	1.512	0.847
	125 – 150 m	26.92	17.07	1.904	-0.161	2.065	0.634
	> 150	9.25	6.21	2.582	-0.059	2.142	0.671

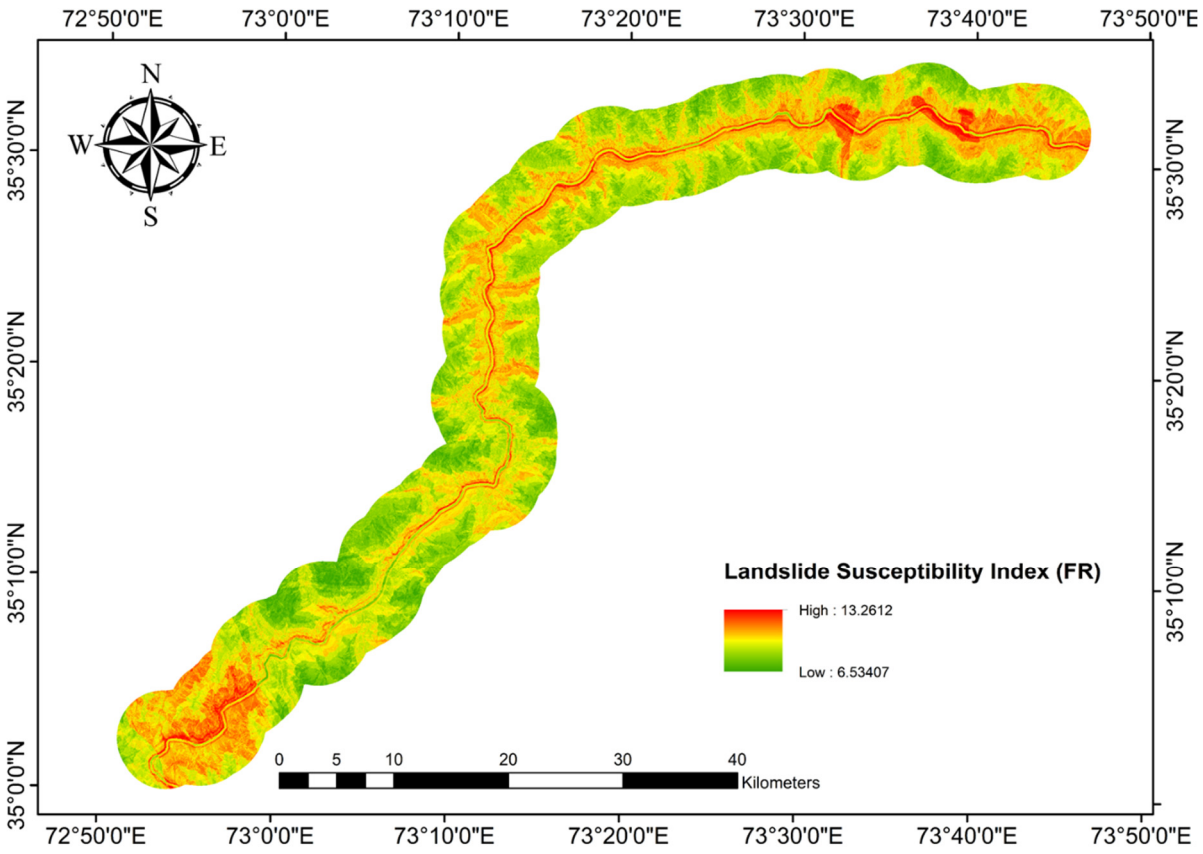

Fig. 9 Landslide susceptibility index produced from FR model.

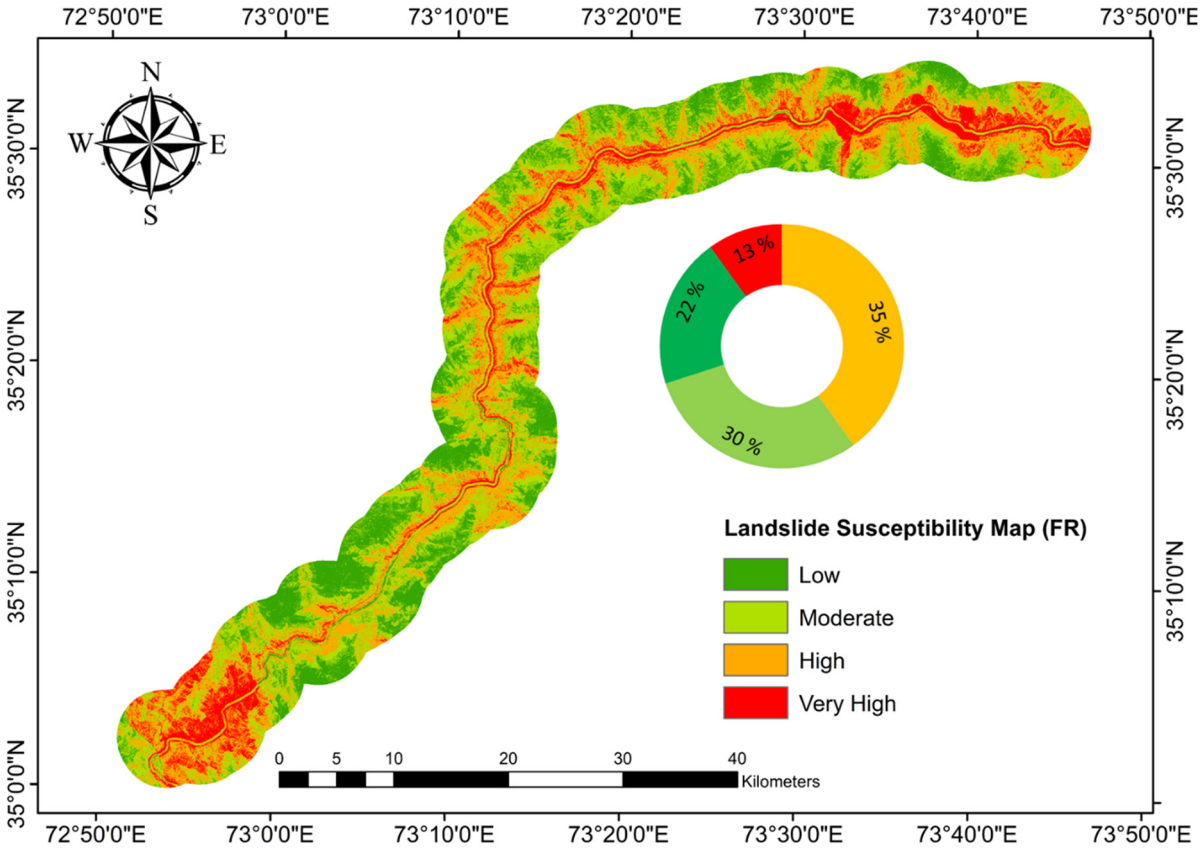

Fig. 10 Landslide susceptibility map produced from FR model.

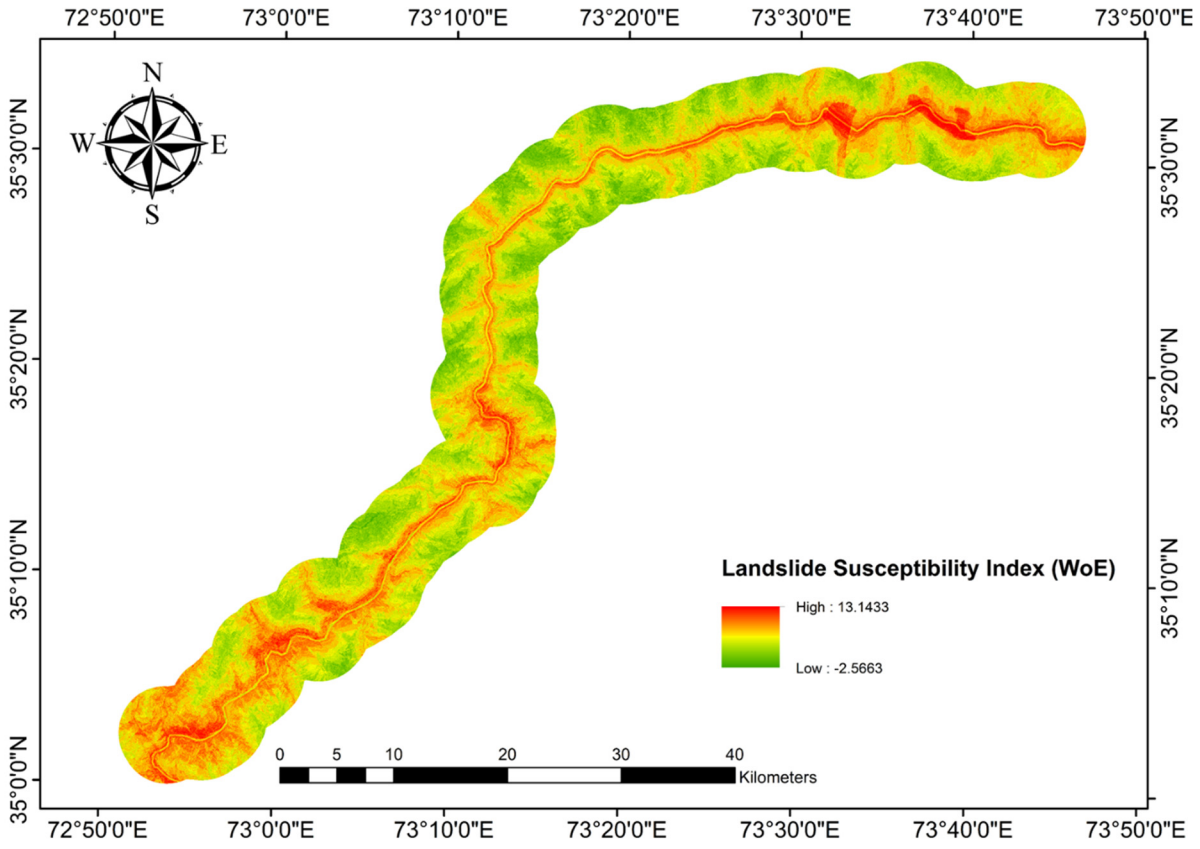

Fig. 11 Landslide susceptibility index produced from WoE model.

Table 2 Contingency table (2x2) where (Ai) observed and (Bi) expected frequencies (Ei) of (L) landslides of F_1 and F_2 binary factors.

		Binary pattern F_1 Present	Absent	Total
Binary pattern F_2	Present	A_1= {$F_1 \cap F_2 \cap L$}	A_3= {$\bar{F_1} \cap F_2 \cap L$}	{$F_2 \cap L$}
		(E_1= {$F_2 \cap L$} *{$F_1 \cap L$}/{L})	(E_3= {$F_2 \cap L$} *{$\bar{F_1} \cap L$}/{L})	
	Absent	A_2= {$F_1 \cap \bar{F_2} \cap L$}	A_4= {$\bar{F_1} \cap \bar{F_2} \cap L$}	{$\bar{F_2} \cap L$}
		(E_2= {$\bar{F_2} \cap L$} *{$F_1 \cap L$}/{L})	(E_4= {$\bar{F_2} \cap L$} *{$\bar{F_1} \cap L$}/{L})	
	Total	{$F_1 \cap L$}	{$\bar{F_1} \cap L$}	{L}

Chi-square values were determined by the following equation

$$x^2 = \sum_{i=1}^{i=n} \frac{(Ai-Bi)}{Bi} \quad (7)$$

The conditional independence between the pairs of the binary pattern of the factors were calculated at 99 % significance level with 1 degree of freedom (6.64) (Table 2). Based on the X^2 predictive value (if X^2 values is then the pair of binary predictor patter is independent), the binary patterns showing conditional independence were included and while those showing conditional dependence were excluded in generation of the landslide susceptibility index and the landslide susceptibility map.

The landslide susceptibility index (LSI) was calculated by addition of all classes C values (Table 1) (Barbieri and Cambuli, 2009). The calculated LSI map values range from -2.56 to 13.14 (Fig. 11). In the LSI map, a higher value corresponds to a higher landslide susceptibility. Furthermore, the LSI map was reclassified into four classes using "natural break" method to get the landslide susceptibility map ((i) low, (ii) moderate, (iii) high, and (iii) very high). Landslide susceptibility map show that 19 % landslides lies in low susceptibility area, 32 % landslide lie in the

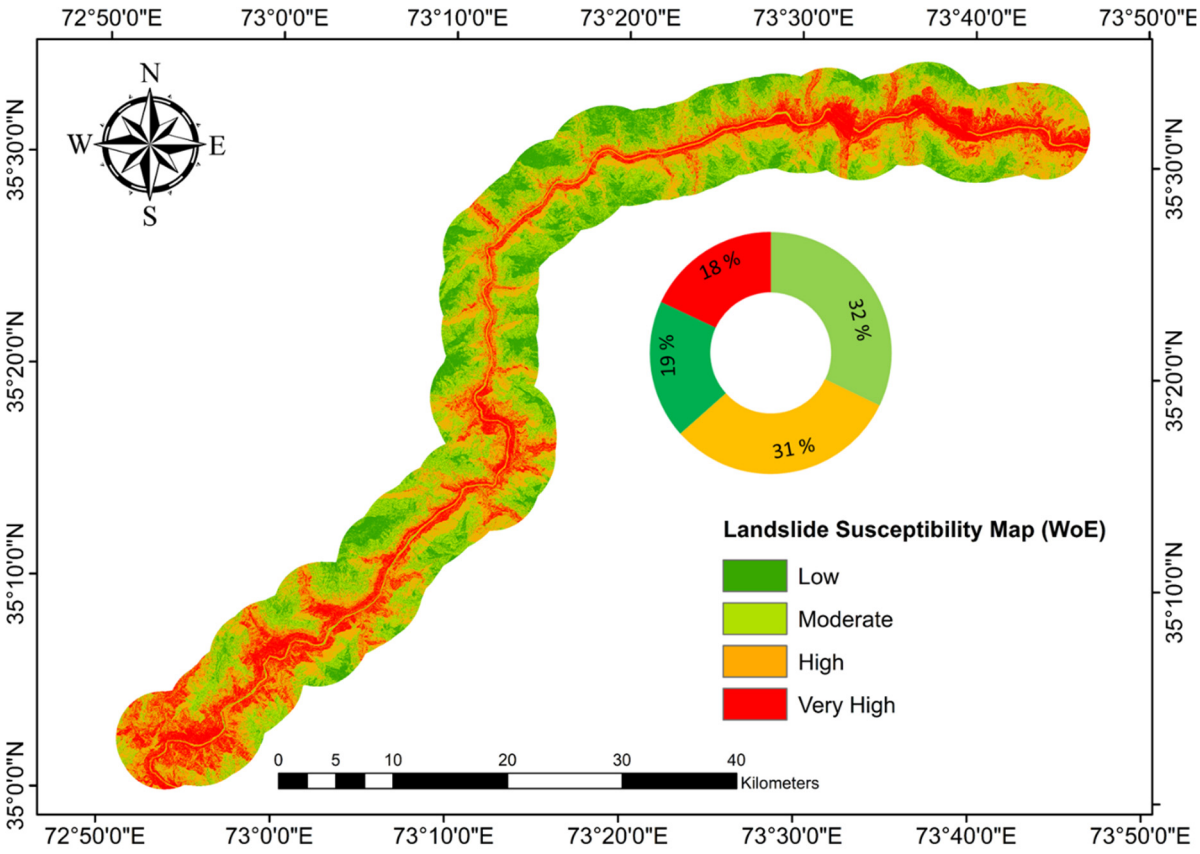

Fig. 12 Landslide susceptibility map produced from WoE model.

moderate susceptibility area, 31 % lie in the high susceptibility area and 18 % lie in the very high susceptibility area (Fig. 12).

VALIDATION OF TWO STATISTICAL BIVARIATE MODELS

Validation is the most important component of landslide susceptibility mapping (Remondo et al., 2003). In order to check the accuracy of model, the area under the curve (AUC) was used to make a quantitative comparison between the two models used in this study (Yesilnacar and Topal, 2005; Beguería, 2006). In validation, the landslides are divided into two datasets (training dataset and the validation dataset). In training dataset, we used the 70 % landslides (725 landslides) by random selection and the remaining 30 % landslides (311 landslides) were used in prediction process (Fig. 13). The training dataset was used to obtain the success rate cure (SRC) while the validation dataset was used to obtain prediction rate curve (PRC) to check the accuracy and reliability of the both models. Hence, the model having the highest AUC is the best. The landslide susceptibility map produced by WoE model gives comparatively better results. To validate the models, the success rate curves (SRC) corresponding to the training dataset as well as prediction rate curve (PRC) corresponding the validation dataset were produced which showed the similar results.

The results of the area under curve (AUC) evaluation gives the values of FR and WoE models as 0.807 and 0.866, respectively; and their corresponding percentages of 80.7 % and 86.6 % respectively (Fig. 14). In addition to this, the AUC values for validation dataset of FR and WoE models were found to be 0.785 and 0.846, respectively; and their corresponding percentages of 78.5 % and 84.6 % respectively (Fig. 15). It is worth mention here that the both model results are consistent with the actual ground situation as observed and investigated during field trips.

DISCUSSION ON RESULTS

Weights-of-evidence (WoE) model has widely been used and well accepted due to consistently good results in landslide susceptibility mapping since last more than one decade (Neuhäuser et al., 2012; Poli and Sterlacchini, 2007; Pourghasemi et al., 2013a, 2013b; Prasannakumar and Vijith, 2012; Regmi et al., 2010; Xu C. et al., 2012a, 2012b). On the other hand frequency ration (FR) model has been used in comparison with other models including artificial neural networks (ANN) model, neuro-fuzzy inference system, logistic regression model, analytical hierarchy process (AHP) model (Chen et al., 2017; Lee and Sambath, 2006; Mondal and Maiti, 2013; Yalcin et al., 2011; Yilmaz, 2009). Many researchers have also compared the WoE model with FR model and have got

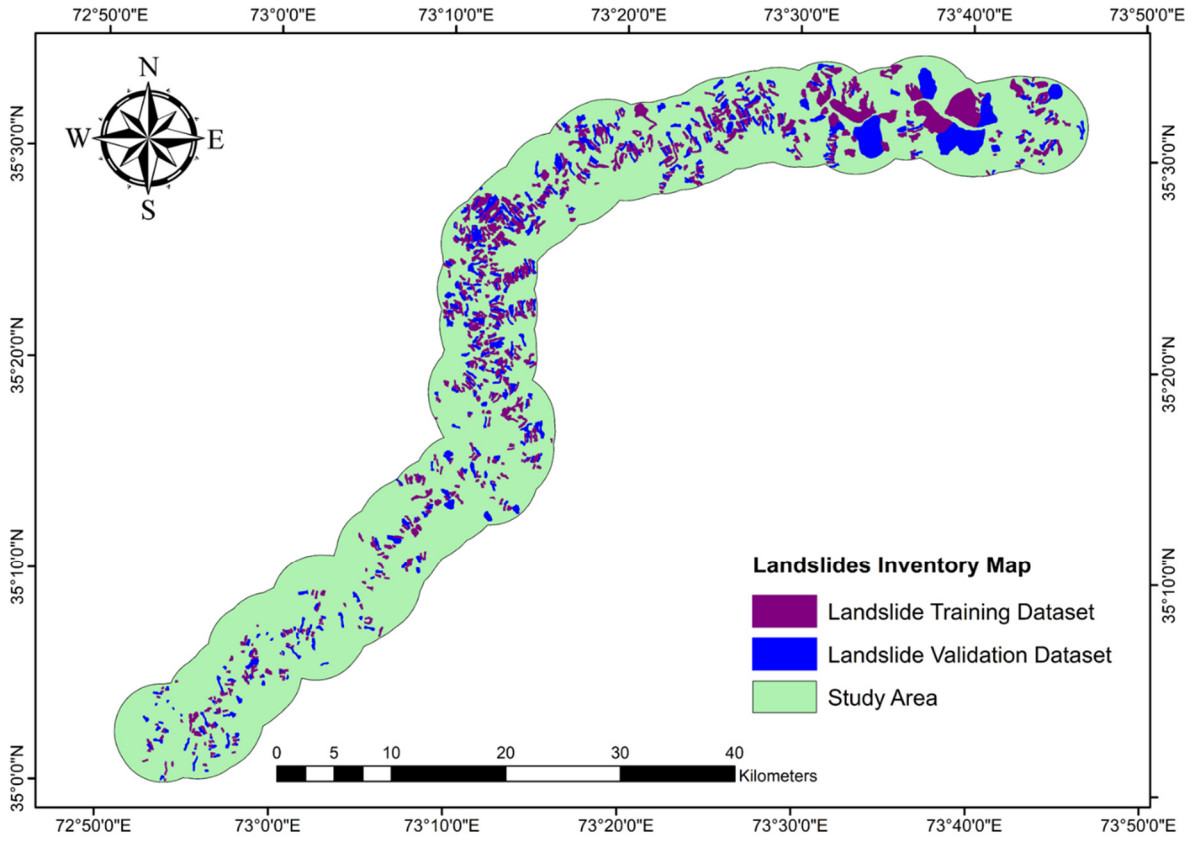

Fig. 13 Landslides training dataset and landslides validation dataset used for susceptibility mapping.

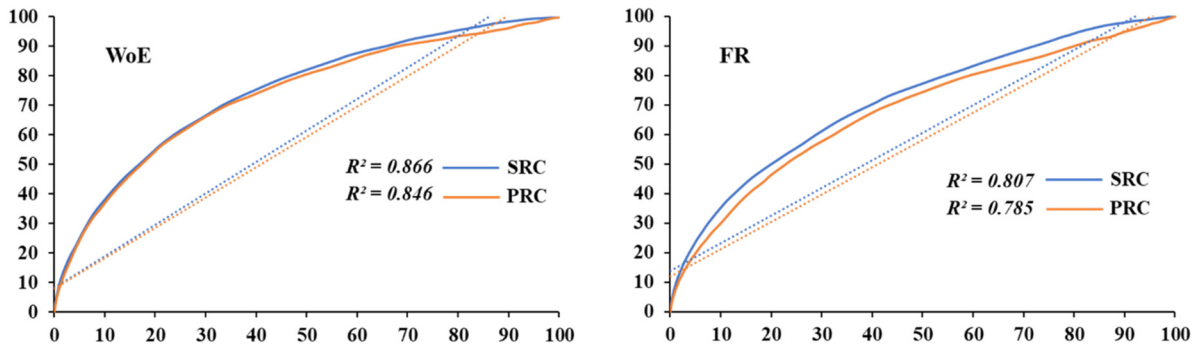

Fig. 14 AUC representing quality of the models: [WoE] success rate ($R^2 = 0.866$) and prediction rate ($R^2 = 0.846$), [FR] success rate ($R^2 = 0.807$) and prediction rate ($R^2 = 0.785$).

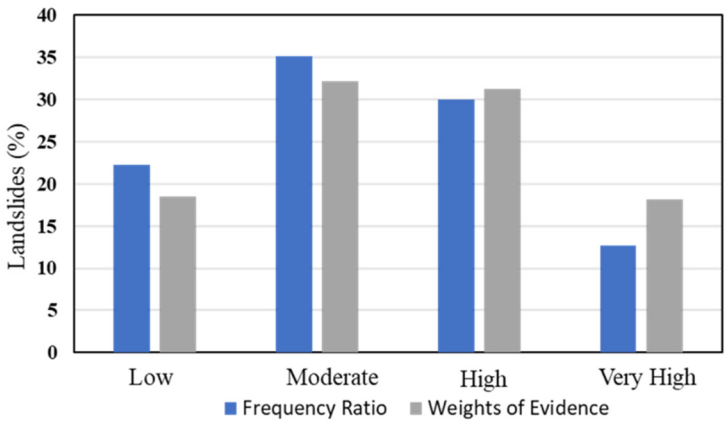

Fig. 15 Comparison of results of FR and WoE models

very satisfactory results having the WoE results slighter higher than the FR results (Ding et al., 2017; Mohammady et al., 2012). In this study we have also used the WoE and FR model for landslide susceptibility mapping and the results were in agreement with the previous studies (WoE have higher accuracy than FR model); however, the overall results of the both models were relatively better than the previous studies especially for FR model.

The triggering mechanisms of landslides are complex and are often unknown for every new location. In this study, landslides were digitized from high resolution GAOFEN-I satellite images as well as from google earth imaginaries followed by field check. On the bases of field survey, remote sensing data as well as the geological data, eleven conditioning factors were selected for susceptibility mapping. The conditioning factors were selected based on availability of data, its relevance as well as the scale of the data. These conditioning factors include slope angle, elevation, slope aspect, plan-curvature, profile-curvature, faults buffer, rivers buffer, roads buffer, NDVI, lithology and relative relief. The ArcGIS was used for making the thematic layers as well as the final susceptibility maps. In both models, similar conditioning factors were used to produce the susceptibility maps so that the results can be compared quantitatively.

It is common observation that landslide occurrence increases with increase in elevation and slope angles. However, the results of this study show that landslides activity decreases with increase in elevation and thus slope angle. It is mainly because of the reason that high altitude areas as well as steep slopes are at larger distance from the KKH which is the main contributing factor in landslide triggering due to down-slope cutting. Maximum landslides occurred within the slope range of 30-40°, it is mostly due to local variations in conditions (Ayalew and Yamagishi, 2005), which may include excessive rainfall, human activities including downslope cutting due to highway construction etc. Results show that the maximum landslides in Hunza-Nagar valley, northern Pakistan were found within the slopes having amount of dip ranging from 30°-50° (Bacha et al. 2018; Riaz et al., 2018). In terms of aspect, the slope face of maximum landslides was towards south which is probably because of receiving maximum sunshine in daytimes followed by temperature decrease at night times, and this phenomenon helps in weathering processes which provide base for maximum potential slopes. The south-facing slopes receive maximum amount of sunshine and hence are more susceptible to landsliding (De Guidi, 2013; Ren et al., 2013). In addition to this, vegetation cover is comparatively higher at high elevation and steep slopes due to less human involvement which is the prime factor of deforestation. The bared slopes are easily susceptible to weathering and thus prone to landsliding than the vegetated slopes, as vegetation makes the slope stability higher than the bared slopes due to the roots enforcement within the soils and rocks of slope material (Malek et al., 2015; Reichenbach et al., 2014). In term of rivers and roads distance, it is found that landslides activity decreases with increase in distance; it is because of less chances of downslope-cutting away from KKH (as per common experience, highways are best known for downslope-cutting in hilly areas). Similar results were found in previous studies (Regmi et al., 2010; Ding et al., 2017). However, the case was slightly different for faults distance. Nevertheless, landslides were concentrated around the faults and were rapidly decreasing with distance (Bacha et al., 2018); however, near Sazin and Dudishal area the landslide activity was found very high even there is no major fault in that area, and this is maybe due to either glacier activity (as there large old landslides deposits that maybe the moraine deposits) or due change in lithology in that area (as maximum landslides were found in Chilas-complex lithology which is present in this area); lithology is one of the most important parameters to determine the occurrence of landsliding in northwest Himalayas in Pakistan (Riaz et al., 2018). In addition to this, Mansehra granite seems to be most stable while the maximum landslides were found in Chilas-complex (61.7 %) followed by Kamila amphibolites (22.9 %). The faults and the relative relief have the more affect than the lithology (Regmi et al., 2010), it is possibly due to the presence of hard rocks in the entire area, with exception of Quaternary deposits and the rocks which are subjected to the high tectonic stresses (e.g., shear zones and fault zones including MMT etc.). In the current study, the relative relief vale of greater than 75 m shows high weights. It was observed that the maximum contrast value (1.18) was found from 25 m to 50 m; however, the maximum landslides activity was found in the range of 75–100 m which makes a faire relation with the landslide occurrence. Although rainfall also affects the landslides especially the debris flows, however due to the unavailability of the reliable rainfall data, it was not included in this study.

The area under the curve (AUC) was to quantitatively compare the both models used in this study. The predictive ability of AUC values indicates that the success rates of FR model and WoE model are 0.807 and 0.866, with corresponding percentages of 80.7 % and 86.6 %, whereas the prediction rates are 0.785 and 0.846, with corresponding percentages of 78.5 % and 84.6 %, respectively. The results of the both models are in agreement with the previous studies using the similar models in other regions (Ding et al., 2017; Mohammady et al., 2012). It is worth mention here that nearly 50 % landslides in the study area were found in either high or very high susceptibility zones by both models results.

Although, both models show relatively good results; however, there is still room to get more reliable results. Hence, it is suggested to use all the other susceptibility methods to get better results if possible, in this study area.

CONCLUSIONS

Based on the detailed investigations along the Dubair-Dudishal section (about 150 km) of the KKH within a buffer zone of 8 km, the following conclusions are drawn;

1. The predictive ability of AUC values indicates that the success rates of FR model and WoE model are 80.7 % and 86.6 %, whereas the prediction rates are 78.5 % and 84.6 %, respectively. Hence, WoE model performs better than the FR model in the study area.
2. Nearly 50 % landslides in the study area were found in either high or very high susceptibility zones based on the results of the models used in this study. Hence, proper mitigation strategy including retaining walls, removal of overburden as well as the continuous monitoring should be done for the whole area especially for the potential slopes to avoid any mishap.
3. These results would be of great importance to the policy makers and the engineers for highway construction as well as the mega dams construction projects (Dasu dam and Bhasha dam which lie within the vicinity of the study area); so that proper prevention as well as mitigation could be done in advance to avoid the possible economic as well as the human loss in future.
4. As this section (study area) is susceptible to landsiding; hence, diverse investigations using of all available susceptibility mapping techniques as well as in-depth study with respect to tectonic and lithological control should be done if possible.

DATA AVAILABILITY STATEMENT

All data, models, and code generated or used during the study appear in the submitted article.

ACKNOWLEDGEMENT

This work is supported by Chinese Academy of Sciences President's International Fellowship Initiative (grant No. 2021VCB0003) and International Partnership Program of Chinese Academy of Sciences (grant No. 131551KYSB20160002). KKH road log prepared by Geological Survey of Pakistan (2010) was used to generate the lithology layer for analysis.

REFERENCES

Agliardi, F., Crosta, G.B. and Frattini, P.: 2012, Slow rock-slope deformation. In: Clague, J.J., Stead, D. (eds), Landslides types, mechanisms and modeling. Cambridge University Press, Cambridge, 207–221.

Agliardi, F., Crosta, G.B. and Zanchi, A.: 2001, Structural constrains on deep-seated slope deformations kinematics. Eng. Geol., 59, 1-2, 83–102. DOI: 10.1016/S0013-7952(00)00066-1

Akgun, A.: 2012, A comparison of landslide susceptibility maps produced by logistic regression, multi-criteria decision, and likelihood ratio methods: a case study at İzmir, Turkey. Landslides, 9, 1, 93–106. DOI: 10.1007/s10346-011-0283-7

Ali, S., Biermanns, P., Haider, R. and Reicherter, K.: 2019, Landslide susceptibility mapping by using a geographic information system (GIS) along the China–Pakistan Economic Corridor (Karakoram Highway), Pakistan, Nat. Hazards Earth Syst. Sci., 19, 999–1022. DOI: 10.5194/nhess-19-999-2019

Ali, S., Haider, R., Abbas, W., Basharat, M. and Reicherter, K.: 2021, Empirical assessment of rockfall and debris flow risk along the Karakoram Highway, Pakistan. Nat. Hazards. DOI: 10.1007/s11069-021-04549-4

Armaş, I.: 2012, Weights of evidence method for landslide susceptibility mapping. Prahova Subcarpathians, Romania. Nat. Hazards, 60, 3, 937–950. DOI: 10.1007/s11069-011-9879-4

Ayalew, L. and Yamagishi, H.: 2005, The application of GIS-based logistic regression for landslide susceptibility mapping in the Kakuda-Yahiko Mountains, Central Japan. Geomorphology, 65, 1-2, 15–31. DOI: 10.1016/j.geomorph.2004.06.010

Ayalew, L., Yamagishi, H. and Ugawa, N.: 2004, Landslide susceptibility mapping using GIS-based weighted linear combination, the case in Tsugawa area of Agano River, Niigata Prefecture, Japan. Landslides, 1, 73–81. DOI: 10.1007/s10346-003-0006-9

Bacha, A.S., Shafique, M. and van der Werff, H.: 2018, Landslide inventory and susceptibility modelling using geospatial tools, in Hunza-Nagar valley, northern Pakistan. J. Mt. Sci., 15, 6, 1354-1370. DOI: 10.1007/s11629-017-4697

Barbieri, G. and Cambuli, P.: 2009, The weight of evidence statistical method in landslide susceptibility mapping of the Rio Pardu Valley (Sardinia, Italy). 18th World IMACS/MODSIM Congress, Cairns, Australia. 13–17 July 2009.

Barredo, J.I., Hervas, J., Lomoschitz, A., Benavides, A., Van, W.C.: 2000, Landslide hazard assessment using GIS and multi-criteria evaluation techniques in the Tirajana Basin, Gran Canaria Island. 5th EC GIS Workshop.

Basharat, M., Shah, H.R. and Hameed, N: 2016, Landslide susceptibility mapping using GIS and weighted overlay method: a case study from NW Himalayas, Pakistan. Arab. J. Geosci., 9, 4, 292. DOI: 10.1007/s12517-016-2308-y

Beguería, S.: 2006, Validation and evaluation of predictive models in hazard assessment and risk management. Nat. Hazards, 37, 3, 315–329. DOI: 10.1007/s11069-005-5182-6

Burbank, D.W., Leland, J., Fielding, E., Anderson, R.S., Brozovic, N., Reid, M.R. and Duncan, C.: 1996, Bedrock incision, rock uplift and threshold hillslopes in the northwestern Himalayas. Nature, 379, 505–510. DOI: 10.1038/379505a0

Butler, R.W.H. and Prior, D.J.: 1988, Anatomy of a continental subduction zone: the main mantle thrust in Northern Pakistan. Geol. Rundschau, 77, 1, 239–255.

Carranza, E.J.M. and Hale, M.: 2001, Geologically constrained probabilistic mapping of gold potential, Baguio district, Philippines. Nat. Resour. Res., 10, 237–253. DOI: 10.1023/A:1011500826411

Chen, W., Pourghasemi, H.R., Panahi, M., Kornejady, I., Wang, J., Xie, X. and Cao, S.: 2017, Spatial prediction of landslide susceptibility using an adaptive neuro-fuzzy inference system combined by frequency ratio, generalized additive model, and support vector machine techniques. Geomorphology, 297, 69–85. DOI: 10.1016/j.geomorph.2017.09.007

Chung, C-J.F. and Fabbri, A.: 2003, Validation of spatial prediction models for landslide hazard mapping. Nat Hazards, 30, 451–472. DOI: 10.1023/B:NHAZ.0000007172.62651.2b

Clift, P.D., Hannigan, R., Blusztajn, J. and Draut, A.E.: 2002, Geochemical evolution of the Dras-Kohistan arc during collision with Eurasia: Evidence from the Ladakh Himalayas, India. Isl. Arc, 11, 4, 255–271. DOI: 10.1046/j.1440-1738.2002.00371.x

Cruden, D.M. and Varnes, D.J.: 1996, Landslide types and processes. Special Report. Transportation Research Board, National Academy of Sciences, 247, 36–75.

Dahal, R.K., Hasegawa, S., Nonomura, A., Yamanaka, M., Masuda, T. and Nishino, K.: 2008, GIS-based weights-of-evidence modelling of rainfall-induced landslides in small catchments for landslide susceptibility mapping. Environ. Geol., 54, 2, 311–324. DOI: 10.1007/s00254-007-0818-3

Dai, F.C. and Lee, C.F.: 2002, Landslide characteristics and slope instability modeling using GIS, Lantau Island, Hong Kong. Geomorphology, 42, 213–228. DOI: 10.1016/S0169-555X(01)00087-3

Dai, F.C., Lee, C.F., Li, J. and Xu, Z.W.: 2001, Assessment of landslide susceptibility on the natural terrain of Lantau Island, Hong Kong. Environ. Geol., 43, 381–391. DOI: 10.1007/s002540000163

Davis, D., Suppe, J. and Dahlen, F.A.: 1983, Mechanics of fold-and-thrust belts and accretionary wedges. J. Geophys. Res., Solid Earth, 88, B2, 1153–1172. DOI: 10.1029/JB088iB02p01153

De Guidi, G.: 2013, Landslide susceptibility assessment in the Peloritani Mts. (Sicily, Italy) and clues for tectonic control of relief processes. Nat. Hazards Earth Syst. Sci., 13, 4, 949–963. DOI: 10.5194/nhess-13-949-2013

Ding, Q., Chen, W. and Hong, H.: 2017, Application of frequency ratio, weights of evidence and evidential belief function models in landslide susceptibility mapping. Geocarto Int., 32, 6, 619–639. DOI: 10.1080/10106049.2016.1165294

Ding, L., Qasim, M., Jadoon, I.A.K., Khan, M.A., Xu, Q., Cai, F., Wang, H., Baral, U. and Yue, Y.: 2016, The India–Asia collision in north Pakistan: Insight from the U–Pb detrital zircon provenance of Cenozoic foreland basin. Earth Planet. Sci. Lett., 455, 49–61. DOI: 10.1016/j.epsl.2016.09.003

Dramis, F. and Sorriso-Valvo, M.: 1994, Deep-seated gravitational slope deformations, related landslides, and tectonics. Eng. Geol., 38, 3-4, 231–243. DOI: 10.1016/0013-7952(94)90040-X

Du, G.L., Zhang, Y.S., Iqbal, Y., Yang Z.H. and Yao, X.: 2017, Landslide susceptibility mapping using an integrated model of information value method and logistic regression in the Bailongjiang watershed, Gansu Province, China. J. Mt. Sci., 14, 2, 249–268. DOI: 10.1007/s11629-016-4126-9

Emmanuel J, Carranza M, Hale M (2000) Geologically constrained probabilistic mapping of gold potential, Baguio district, Philippines. Nat Resour Res, 9, 237–253.

Ercanoglu, M. and Gokceoglu, C.: 2002, Assessment of landslide susceptibility for a landslide-prone area (north of Yenice, NW Turkey by fuzzy approach. Environ. Geol., 41, 720–730. DOI: 10.1007/s00254-001-0454-2

Fraser, D.F., Gilliam, J.F., Daley, M.J., Le, A.N. and Skalski, G.T.: 2001, Explaining leptokurtic movement distributions: Intrapopulation variation in boldness and exploration. Am. Nat., 158, 2. DOI: 10.1086/321307

Gorum, T., Fan, X., van Westen, C.J., Huang, R.Q., Xu, Q., Tang, C. and Wang, G.: 2011, Distribution pattern of earthquake-induced landslides triggered by the 12 May 2008 Wenchuan earthquake. Geomorphology, 133, 152–167. DOI: 10.1016/j.geomorph.2010.12.030

Hanson, C.R: 1989, The northern suture in the Shigar Valley, Baltistan, northern Pakistan, in Malinconico, L.L.J. and Lillie, R.J., eds., Tectonics of the Western Himalayas: Geological Society of America, Special Paper, 232, 203–215.

Iqbal, J., Dai, F., Hong, M. and Tu, X.: 2018, Failure mechanism and stability analysis of an active landslide in the Xiangjiaba reservoir area, South-west China. J. Earth Sci., 29, 3, 646–661. DOI: 10.1007/s12583-017-0753-5

Iqbal, J., Tu, X. and Xu. L.: 2017, Landslide hazards assessment in the reservoir areas. A case study of Xiangjiaba Reservoir, Southwest China. Nat. Hazards Rev., 18, 4. DOI: 10.1061/(ASCE)NH.1527-6996.0000245

Jadoon, I.A.K., Hinderer, M., Kausar, A.B. and Frisch, W.: 2015, Structural interpretation and geo-hazard assessment of a locking line: 2005 Kashmir earthquake, western Himalayas. Environ. Earth Sci., 73, 11, 587–7602. DOI: 10.1007/s12665-014-3929-7

Justice, C.O., Townshend, J.R.G., Holben, B.N. and Tucker, E.C.: 1985, Analysis of the phenology of global vegetation using meteorological satellite data. Int. J. Remote Sens., 6, 1271–1318. DOI: 10.1080/01431168508948281

Khan, T., Khan, M.A., Jan, M.Q. and Naseem, M.: 1996, Back-arc basin assemblages in Kohistan, Northern Pakistan. Geodin. Acta, 9, 30–40. DOI: 10.1080/09853111.1996.11417261

Larsen, I.J. and Montgomery, D.R.: 2012, Landslide erosion coupled to tectonics and river incision. Nat. Geosci., 5, 468–473. DOI: 10.1038/ngeo1479

Lee, S., Choi, J. and Min, K.: 2004, Probabilistic landslide hazard mapping using GIS and remote sensing data at Boun, Korea. Int. J. Remote Sens., 25, 11, 2037–2052. DOI: 10.1080/01431160310001618734

Lee, S. and Pradhan, B.: 2007, Landslide hazard mapping at Selangor, Malaysia using frequency ratio and logistic regression models. Landslides, 4, 33–41. DOI: 10.1007/s10346-006-0047-y

Lee, S. and Sambath, T.: 2006, Landslide susceptibility mapping in the Damrei Romel area, Cambodia using frequency ratio and logistic regression models. Environ. Geol., 50, 847–855. DOI: 10.1007/s00254-006-0256-7

Lee, S. and Talib, J.A.: 2005, Probabilistic landslide susceptibility and factor effect analysis. Environ. Geol., 47, 982–990. DOI: 10.1007/s00254-005-1228-z

Li, L., Yao, X., Zhang, Y., Iqbal, J., Chen, J. and Zhou, N.: 2016, Surface recovery of landslides triggered by 2008 Ms 8.0 Wenchuan earthquake (China): a case study in a typical mountainous watershed. Landslides, 13, 4, 787–794. DOI: 10.1007/s10346-015-0594-1

Malek, Ž., Zumpano, V., Schröter, D. et al.: 2015, Scenarios of land cover change and landslide susceptibility: An example from the Buzau Subcarpathians, Romania. In: Lollino, G., Manconi, A., Guzzetti, F. et al. (eds.),

Engineering Geology for Society and Territory, vol. 5. Springer International Publishing. 743–746. DOI: 10.1007/978-3-319-09048-1_144

Mohammady, M., Pourghasemi, H.R. and Pradhan, B.: 2012, Landslide susceptibility mapping at Golestan Province, Iran: a comparison between frequency ratio, Dempster–Shafer, and weights-of-evidence models. J. Asian Earth Sci., 61, 221–236. DOI: 10.1016/j.jseaes.2012.10.005

Mondal, S. and Maiti, R.: 2013, Integrating the analytical hierarchy process (AHP) and the frequency ratio (FR) model in landslide susceptibility mapping of Shivkhola watershed, Darjeeling Himalaya. Int. J. Disaster Risk Sci., 4, 4, 200–212. DOI: 10.1007/s13753-013-0021-y

Morley, C.K.: 1988, Out-of-sequence thrusts. Tectonics, 7, 3, 539–561. DOI: 10.1029/TC007i003p00539

Nefeslioglu, H.A., Duman, T.Y. and Durmaz, S.: 2008, Landslide susceptibility mapping for a part of tectonic Kelkit Valley (Eastern Black Sea region of Turkey). Geomorphology, 94, 3-4, 401–418. DOI: 10.1016/j.geomorph.2006.10.036

Neuhäuser, B., Damm, B. and Terhorst, B.: 2012, GIS-based assessment of landslide susceptibility on the base of the weights-of-evidence model. Landslides, 9, 4, 511–528. DOI: 10.1007/s10346-011-0305-5

Neuhäuser, B. and Terhorst, B.: 2007, Landslide susceptibility assessment using "weights-of-evidence" applied to a study area at the Jurassic escarpment (SW-Germany). Geomorphology, 86, 1-2, 12–24. DOI: 10.1016/j.geomorph.2006.08.002

Peruccacci, S., Brunetti, M.T., Luciani, S., Vennari, C. and Guzzetti, F.: 2012, Lithological and seasonal control of rainfall thresholds for the possible initiation of landslides in central Italy. Geomorphology, 139-140, 79–90. DOI: 10.1016/j.geomorph.2011.10.005

Poli, S. and Sterlacchini, S.: 2007, Landslide representation strategies in susceptibility studies using weights-of-evidence modeling technique. Nat. Resour. Res., 16, 2, 121–134. DOI: 10.1007/s11053-007-9043-8

Pourghasemi, H.R., Gayen, A., Park, S., Lee, C.W. and Lee, S.: 2018a, Assessment of landslide prone areas and its zonation using Logistic Regression, LogitBoost, and NaïveBayes Machine Learning Algorithms. Sustainability, 10, 10, 3697. DOI: 10.3390/su10103697

Pourghasemi, H.R., Pradhan, B., Gokceoglu, C. and Moezzi, K.D.: 2013a, A comparative assessment of prediction capabilities of Dempster–Shafer and weights-of-evidence models in landslide susceptibility mapping using GIS. Geomat. Nat. Haz. Risk, 4, 93–118. DOI: 10.1080/19475705.2012.662915

Pourghasemi, H.R., Pradhan, B., Gokceoglu, C., Mohammadi, M. and Moradi, H.R.: 2013b, Application of weight-sof-evidence and certainty factor models and their comparison in landslide susceptibility mapping at Haraz Watershed, Iran. Arab. J. Geosci., 6, 7, 2351–2365. DOI 10.1007/s12517-012-0532-7

Pourghasemi, H.R., Timoori Yansari, Z., Panagos, P. and Pradhan, B: 2018b, Analysis and evaluation of landslide susceptibility: A review on articles published during 2005-2016 (periods of 2005-2012 and 2013-2016). Arab. J. Geosci., 11, 193. DOI: 10.1007/s12517-018-3531-5

Pradhan, B.: 2013, A comparative study on the predictive ability of the decision tree, support vector machine and neuro-fuzzy models in landslide susceptibility mapping using GIS. Comput. Geosci., 51, 350–365. DOI: 10.1016/j.cageo.2012.08.023

Pradhan, B., Oh, H.-J., Buchroithner, M.: 2010, Weights-of-evidence model applied to landslide susceptibility mapping in a tropical hilly area. Geomat. Nat. Haz. Risk, 1, 3, 199–223. DOI: 10.1080/19475705.2010.498151

Pradhan, B., Youssef, A. and Varathrajoo, R.: 2010, Approaches for delineating landslide hazard areas using different training sites in an advanced artificial neural network model. Geo-spat. Inf. Sci., 13, 93–102. DOI: 10.1007/s11806-010-0236-7

Prasannakumar, 0.V. and Vijith, H.: 2012, Evaluation and validation of landslide spatial susceptibility in the Western Ghats of Kerala, through GIS-Bsed Weights of Evidence Model and area under curve technique. J. Geol. Soc. India, 80, 4, 515–523. DOI: 10.1007/s12594-012-0171-3

Regmi, N.R., Giardino, J.R. and Vitek, J.D.: 2010, Modeling susceptibility to landslides using the weight of evidence approach: Western Colorado, USA. Geomorphology, 115, 1-2, 172–187. DOI: 10.1016/j.geomorph.2009.10.002

Reichenbach, P., Busca, C., Mondini, A.C. and Rossi, M.: 2014, The influence of land use change on landslide susceptibility zonation: the Briga Catchment test site (Messina, Italy). Environ. Manage., 54, 6, 1372–1384. DOI: 10.1007/s00267-014-0357-0

Remondo, J., González-Diez, A., de Terán, J.R.D. and Cendrero, A.: 2003, Landslide susceptibility models utilizing spatial data analysis techniques: a case study from the Lower Deba Valley, Guipu´zcoa (Spain). Nat. Hazards, 30, 3, 267–279. DOI: 10.1023/B:NHAZ.0000007202.12543.3a

Ren, Z., Zhang, Z., Dai, F., Yin, J. and Zhang H.: 2013, Co-seismic landslide topographic analysis based on multi-temporal DEM—A case study of the Wenchuan earthquake. SpringerPlus,2, 1, 544. DOI: 10.1186/2193-1801-2-544

Rezaei Moghaddam, M.H., Khayyam, M., Ahmadi, M. and Farajzadeh, M.: 2007, Mapping susceptibility landslide by using the weight-of-evidence model: a case study in Merek Valley, Iran. J. Appl. Sci., 7, 22, 3342–3355. DOI: 10.3923/jas.2007.3342.3355

Riaz, M.T., Basharat, M., Hameed, N., Shafique, M. and Luo, J.: 2018, A data-driven approach to landslide-susceptibility mapping in mountainous terrain: Case study from the northwest Himalayas, Pakistan. Nat. Hazards Rev., 19, 4. DOI: 10.1061/(ASCE)NH.1527-6996.0000302

Rupke, J., Cammeraat, E., Seijmonsbergen, A.C. and Van Westen, C.J.: 1988, Engineering geomorphology of the Widentobel catchment, Switzerland: a geomorphological inventory system applied to geotechnical appraisal of the slope stability. Eng. Geol., 26, 33–68. DOI: 10.1016/0013-7952(88)90005-1

Saadatkhah, N., Kassim, A. and Lee, L.M.: 2014, Susceptibility assessment of shallow landslides in Hulu Kelang area, Kuala Lumpur, Malaysia using analytical hierarchy process and frequency ratio. Geotech. Geol. Eng., 33, 43–57. DOI: 10.1007/s10706-014-9818-8

Schmidt, K.M. and Montgomery, D.R.: 1995, Limits to relief. Science, 270, 5236, 617–620. DOI: 10.1126/science.270.5236.617

Searle, M.P., Khan, M.A., Fraser, J.E., Gough, S.J. and Jan, M.Q.: 1999, The tectonic evolution of the Kohistan - Karakoram collision belt along the Karakoram Highway transect, north Pakistan, Tectonics, 18, 6, 929–949. DOI: 10.1029/1999TC900042

Süzen, M.L. and Doyuran, V. A.: 2004, comparison of the GIS based landslide susceptibility assessment methods: multivariate versus bivariate. Env. Geol., 45, 665–679. DOI: 10.1007/s00254-003-0917-8

Tahirkheli, R.A.K. and Jan, M.Q.: 1979, Geology of Kohistan, Karakorum Himalaya, northern Pakistan. Geol. Bull. Univ., Peshawar, Pakistan, 11, 1–30.

Tahirkheli, R.A.K., Mattauer, M., Proust, F. and Tapponnier, P.: 1979, The India-Eurasia suture zone in northern Pakistan; synthesis and interpretation of recent data atplate scale. In: Farah, A., De Jong, K.A. (Eds.), Geodynamics of Pakistan. Geological Survey of Pakistan, 125–130.

Treloar, P.J., O'Brien, P.J., Parrish, R.R. and Khan, M.A.: 2003, Exhumation of early Tertiary, coesite-bearing eclogites from the Pakistan Himalaya. J. Geol. Soc. London, 160, 367–376. DOI: 10.1144/0016-764902-075

Treloar, P.J.: 1997, Thermal controls on early-Tertiary, shortlived, rapid regional metamorphism in the NW Himalaya, Pakistan. Tectonophysics, 273, 1, 77–104. DOI: 10.1016/S0040-1951(96)00289-2

Treloar, P.J., Petterson, M.G., Jan, M.Q. and Sullivan, M.A.: 1996, A re-evaluation of the stratigraphy and evolution of the Kohistan arc sequence, Pakistan Himalaya: Implications for magmatic and tectonic arc building processes: J. Geol. Soc. London, 153, 5, 681–693. DOI: 10.1144/gsjgs.153.5.0681

Treloar, P.J., Rex, B.C., Guise, P.G., Coward, M.P., Searle, M.P., Windley, B.F., Petterson, M.G., Jan, M.Q. and Luff, I.W.: 1989, K–Ar and Ar–Ar geochronology of the Himalayan collision in NW Pakistan: Constraints on the timing of suturing, deformation, metamorphism and uplift. Tectonics, 8, 881–909.

Van Westen, C.J.: 2000, The Modelling of Landslide Hazards Using GIS. Surv. Geophys., 21, 2-3, 241–255.

Van Westen, C., van Asch, T. and Soeters, R.: 2006, Landslide hazard and risk zonation—why is it still so difficult? Bull. Eng. Geol. Environ., 65, 167–184. DOI: 10.1007/s10064-005-0023-0

Van Westen, C.J., Rengers, N. and Soeters, R.: 2003, Use of geomorphological information in indirect landslide susceptibility assessment. Nat. Hazards, 30, 3, 399–419. DOI: 10.1023/B:NHAZ.0000007097.42735.9e

Varnes, D.J.: 1978, Slope movements types and processes, In Schuster, R. L. and Krizek, R. J. (Eds.), Landslides analysis and control, Washington, D.C., USA.

Vijith, H., Krishnakumar, K.N., Pradeep, G.S., Ninu Krishnan, M.V. and Madhu, G.: 2014, Shallow landslide initiation susceptibility mapping by GIS-based weights-of-evidence analysis of multi-class spatial data-sets: a case study from the natural sloping terrain of Western Ghats, India. Georisk: Assessment and Management of Risk for Engineered Systems and Geohazards, 8, 1, 48–62. DOI: 10.1080/17499518.2013.843437

Xiangjiaba Reservoir, Southwest China. Nat. Hazards Rev., 18, 4. DOI: 10.1061/(ASCE)NH.1527-6996.0000245

Xu, L., Dai, F.C., Chen, J., Iqbal, J. and Qu, Y.: 2014, Analysis of a progressive slope failure in the Xiangjiaba reservoir area, Southwest China. Landslides, 11, 1, 55–66. DOI: 10.1007/s10346-012-0373-1

Xu, C., Xu, X., Dai, F., Xiao, J., Tan, X. and Yuan, R.: 2012a, Landslide hazard mapping using GIS and weight of evidence model in Qingshui River watershed of 2008 Wenchuan earthquake struck region. J. Earth Sci., 23, 97–120. DOI: 10.1007/s12583-012-0236-7

Xu, C., Xu, X., Lee, Y.H., Tan, X., Yu, G. and Dai, F.: 2012b, The 2010 Yushu earthquake triggered landslide hazard mapping using GIS and weight of evidence modeling. Environ. Earth Sci., 66, 1603–1616. DOI: 10.1007/s12665-012-1624-0

Yalcin, A., Reis, S., Aydinoglu, A.C. and Yomralioglu, T.: 2011, A GIS-based comparative study of frequency ratio, analytical hierarchy process, bivariate statistics and logistics regression methods for landslide susceptibility mapping in Trabzon, NE Turkey. Catena, 85, 274–287. DOI: 10.1016/j.catena.2011.01.014

Yao, X., Tham, L.G. and Dai, F.C.: 2008, Landslide susceptibility mapping based on support vector machine: a case study on natural slopes of Hong Kong, China. Geomorphology, 101, 572–582. DOI: 10.1016/j.geomorph.2008.02.011

Yesilnacar, E. and Topal, T.: 2005, Landslide susceptibility mapping: A comparison of logistic regression and neural networks methods in a medium scale study, Hendek Region (Turkey). Eng. Geol., 79, 3‑4, 251‑266. DOI: 10.1016/j.enggeo.2005.02.002

Yilmaz, I.: 2009, Landslide susceptibility mapping using frequency ratio, logistic regression, artificial neural networks and their comparison: a case study from Kat landslides (Tokat – Turkey). Comput. Geosci., 35, 6, 1125–1138. DOI: 10.1016/j.cageo.2008.08.007

Youssef, A.M., Pourghasemi, H.R., Pourtaghi, Z. and Al-Katheeri, M.M.: 2016, Landslide susceptibility mapping using random forest, boosted regression tree, classification and regression tree, and general linear models and comparison of their performance at Wadi Tayyah Basin, Asir region, Saudi Arabia. Landslides, 13, 839–856. DOI: 10.1007/s10346-015-0614-1

Youssef, A.M., Al-Kathery, M. and Pradhan, B.: 2015, Landslide susceptibility mapping at Al-Hasher area, Jizan (Saudi Arabia) using GIS-based frequency ratio and index of entropy models. Geosci. J., 19, 113–134. DOI: 10.1007/s12303-014-0032-8

Zhou, C., Yin, K., Cao, Y., Ahmed, B., Li, Y., Catani, F and Pourghasemi, H.R.: 2018, Landslide susceptibility modeling applying machine learning methods: A case study from Longju in the Three Gorges Reservoir area, China. Comput. Geosci., 112, 23–37. DOI: 10.1016/j.cageo.2017.11.019